Physics – Uspekhi **39** (11) 1137 – 1156 (1996)

REVIEWS OF TOPICAL PROBLEMS PACS numbers: **52.25.–b, 52.90.+z**

Nonuniform gas discharge plasma

A V Eletskiĭ, B M Smirnov

Contents

Abstract. Formation mechanisms for spatially nonuniform temperature and charged particle density distributions in a low-temperature gas discharge plasma are reviewed. Conditions for the occurrence of, and parameter distributions in, the constricted state of the discharge are analyzed. Spatial temperature and electron density distributions and the pressure and power-input dependence of the plasma column radius are determined in local thermodynamic equilibrium. Special attention is given to a cluster-containing plasma. For this new type of spatially nonuniform discharge plasma, the cluster growth process is studied and the limiting cluster size is evaluated. The potential application of the cluster plasma as an illumination source is assessed and performance characteristics of such a source are calculated.

1. Introduction

Gas discharge plasma comprises the most widely used plasma model, in which the operating conditions are maintained by means of electric current flowing in a gas under the action of an electrical or electromagnetic fields. The region filled with a gas discharge plasma has a limited size and is surrounded either by cooled walls or somewhat cooler gas. In such an object the heat and mass transfer phenomena play an important role. They occur simultaneously with volumetric processes of energy release as well as with charged particles formation and neutralization processes. For these reasons a gas discharge plasma is always distinguished by notably enhanced degree of spatial nonuniformity.

Owing to a complicated kinetics of processes proceeded in a spatially nonuniform gas discharge plasma the latter appears to be quite attractive object of the basic research. The reason is that a great variety of elementary processes proceed on a microscopic level and determine the macroscopic behaviour of a plasma. The results of studies performed in the last few decades show a variety of forms, in which spatial nonuniformities of a gas discharge plasma manifest themselves. The study of mechanisms responsible for transition from one type of a spatial nonuniformity to another is also of considerable scientific interest. Considering the mechanisms of formation of a spatially nonuniform plasma and paths for its transition from one state to another, this physical object can be regarded as a self-organizing system having a large number of degrees of freedom.

The spatial nonuniformity of a gas discharge plasma determines a region of possibilities of its use in devices and installations of practical interest. Thus, the output parameters of powerful gas lasers excited by an electrical discharge are lowered sharply as a result of considerable disturbance in the spatial uniformity of a gas discharge plasma [1 – 3]. The spatial nonuniformity of plasma in gas discharge lighting devices limits the size of a luminous region and as a consequence the light yield of a lamp [4]. As an extreme manifestation of the spatial nonuniformity of plasma it should be mentioned extended condensed structures (clusters), which can be formed within a gas discharge plasma

A V Eletskiĭ Russian Research Center 'Kurchatov Institute'
pl. Kurchatova 1, 123182 Moscow, Russia
Tel. (7-095) 196-72 80. E-mail: avel@bezelst.msk.ru
B M Smirnov Institute for High Temperatures,
Russian Academy of Sciences
ul. Izhorskaya 13/19, 127412 Moskow, Russia
Tel./Fax (7-095) 190-42 22. E-mail: smirnov@termo.msk. su

Received 4 March 1996
Uspekhi Fizicheskikh Nauk **166** (11) 1197–1217 (1996)
Translated by the authors, edited by A Radzig

under certain conditions as a result of condensation of a supersaturated vapor [5 – 7]. These structures are of independent scientific interest. Besides they may be used as the basis for development of a new type of light sources having quite high performance [5 – 7].

Some common features pertaining to a spatially nonuniform gas discharge plasma and specific physical mechanisms governing both the formation conditions and degree of nonuniformity are the concern of this article. In addition, some gas discharge devices of practical interest operating on the basis of a spatially nonuniform plasma have been analyzed. The analysis employs modern data about elementary processes running in a gas discharge plasma and determining the mechanisms for formation and neutralization of charged particles in it.

2. Mechanisms for constriction of a gas discharge

2.1 General

Constriction (contraction) pertains to the most common manifestation of the spatial nonuniformity of a gas discharge. It is a universal physical phenomenon having place in both dc and ac discharges at enhanced pressures or input energies. And it consists in an abrupt change of the discharge operation mode as a result of exceeding some magnitude of gas pressure or discharge current. As a consequence of constriction, the cross section of the region filled with the discharge proves to be much less than the discharge tube radius. Constriction prevents the complete usage of the discharge tube volume, causes a pronounced disturbance in the spatial uniformity of a gas discharge as well as a lowering in the degree of deflection from the equilibrium state. This phenomenon is considered usually as a deleterious one, because it limits from above a range of parameter variation relevant to a gas discharge, which found a wide utility in such devices of high practical importance as plasmotrons, MHD-generators, gaseous lasers, etc.

Gas discharge constriction phenomenon is a subject of both the experimental and theoretical research of long standing, findings of early works being reflected quite fully in reviews and monographs [1, 2, 8 – 11]. There are two important circumstances conditioning our interest to the investigation of this phenomenon. First and foremost, this phenomenon determines the limiting outputs of physical devices and apparatuses of practical interest. As a consequence, both understanding of the constriction mechanisms and knowledge of their quantitative features are necessary for optimizing the performance of the facilities mentioned. However, exploration of gas discharge constriction phenomenon is of interest not only with respect to applications, but also from the viewpoint of basic research. This phenomenon provides one of the illustrative examples for self-organization of a gas discharge plasma which occurs at a macroscopic scale as a result of mutual influence of a number of physical processes proceeding on a microscopic level. The theoretical analysis of those processes has given birth to establishment of several constriction mechanisms differed fundamentally from each other. The possibility of realizing each one depends on the experimental conditions, specifically, on the kind of a gas filling the discharge tube.

In spite of the practical significance of the constriction phenomenon, its experimental investigations have not kept pace with the theoretical ones for years. This can be appreciably explained by the difficulties in measuring the electron radial distribution in the constricted column of a discharge. This circumstance along with a considerable uncertainty in the rate constants of elementary processes determining the character of constriction in a multi-component plasma hindered over many years the detailed quantitative investigation of mechanisms of this phenomena and also the establishment of a relative contribution of each of the processes in specific experimental conditions. Some advance in this direction can be noted in last years owing to the emergence of a considerable number of detailed experimental studies on both the character of the electron density radial distribution in a discharge tube and the conditions which provide the discharge transition into the constricted state. The analysis of these experiments permits a more full picture of phenomena occurring in the positive column of discharge at enhanced currents and pressures to be drawn.

The problem of investigating the gas discharge constriction includes two aspects deserving a special attention. On the one hand, the constriction of a discharge relates to a class of critical phenomena in a low-temperature plasma possessing the instability character. Therewith as a subject of investigation can serve both the conditions for initiating such an instability and the character of system transition from one stable state into another in accordance with external discharge parameters. The main discharge characteristics depend in a rather complicated manner on such parameters as gas pressure and temperature, number density and mean energy of electrons, etc. For this reason the balance equations governing both the electron number density and gas temperature can have in certain situations more than one solution. This means a possibility of existing various modes of radial distribution for electron number density as well as for gas temperature under the same external discharge parameters. Thus, determination of conditions for the discharge constriction is reduced to the problem of stability for the solution of balance equations governing the electron number density and gas temperature in a discharge.

As the second important aspect of the gas discharge constriction problem has to be mentioned the determination of radial distribution for electron number density as well as gas temperature in a constricted discharge. This problem is solved on the basis of simultaneous analysis of nonlinear balance equations for electron number density and gas temperature in a discharge with taking account of the complicated balance of the volumetric and surface processes of charged particles formation and neutralization along with the processes of heat release and removal. The analysis is considerably complicated in the case of discharge in multicomponent gas mixtures, specifically, in the presence of molecular admixtures. This is concerned with the necessity for taking into account the energy stored in vibrational degrees of freedom. When considering below the indicated aspects of the discharge constriction problem, the main attention will be paid to an idea content of the matter. This is turned out to be possible as a result of using the relatively simple physical models.

2.2 Radial distribution of the electron number density in a discharge tube

Balance equation. Let us consider a longitudinal discharge in a long cylindrical tube of radius R_0. The steady-state radial distribution of the electron number density $N_e(r)$ has to be

found as a solution of the balance equation, the most generally employed form of which is the following one:

$$\operatorname{div} D_a \operatorname{grad} N_e + \nu_{ion} N_e - \alpha_{rec} N_e N_i - \gamma N N_e = 0 . \quad (2.1)$$

In this equation, the first term defines the diffusive removal of charged particles to the discharge tube wall (D_a is the ambipolar diffusion coefficient). Such a notation is valid in the case of a quasi-neutral plasma, the transversal size of which is much greater than the Debye radius

$$r_D \simeq \left(\frac{T_e}{8\pi N_e e^2}\right)^{1/2}$$

(T_e is the electron temperature, e is the electron charge). In a gas discharge plasma this condition is obeyed for all practical purposes. The second term in equation (2.1) relates to the volumetric formation of charged particles (ν_{ion} is the ionization frequency on a per-electron basis). It is supposed that the charge particle formation in the discharge is a result of collisions of free electrons with neutral atoms or molecules. Otherwise this form has to be changed. For example, this is the case when the charged particle formation results from collisions with participation of excited atoms (associative ionization or Penning effect). The third term in (2.1) reflects the process of volume neutralization of charged particles (α_{rec} is the recombination coefficient, N_i is the positive ion number density in a discharge). The condition of quasi-neutrality $N_e \approx N_i$ facilitates in a natural manner the form of this term. However, the failure to carry out the indicated condition can be caused not only by the deviation from quasi-neutrality but also by the presence of ions of various kind in a plasma, specifically, negative ions. This can be taken into consideration quite easily through the corresponding change in the form of equation (2.1). The last term in (2.1) describes the process of electron attachment to gas particles (γ is the rate constant for attachment). This formulation can be also modified by considering several various channels of electron attachment as well as possibility for the formation of negative ions of various kind. As boundary conditions, which have to be added to equation (2.1), they require usually that both the electron number density at the discharge tube walls and its radial derivative at the axis are equal to zero:

$$N_e(R_0) = 0 , \quad (2.2)$$

$$\frac{dN_e}{dr}(r = 0) = 0 . \quad (2.3)$$

The sense of those conditions is quite obvious and has no need of some explanations.

Despite an apparent simplicity of equation (2.1), its solution for a constricted discharge meets not only computational but also fundamental difficulties. This is caused by the following circumstances. Firstly, the coefficients of this equation are, in general, radially dependent. This is because of the radial nonuniformities in gas temperature, number densities of charged and excited particles of various kind, electron energy distribution function and, probably, in ionic content of a plasma. For this reason, equation (2.1) is entirely insufficient for determining the radial dependencies of the discharge characteristics involved. At the rigorous formulation of a problem, this equation has to be analyzed in combination with balance equations for excited and charged particles of various kind, heat conduction equation, vibrational energy balance equation and Boltzmann kinetic equation governing the electron energy distribution function. These circumstances considerably complicate mathematical aspects of the problem. In such a situation, analysis of a problem on the basis of consideration of separate simplified models appears to be much more fruitful for establishing the mechanisms of the discharge constriction. In doing so, there is a possibility to reveal the impact of a given factor on the character of solution to equation (2.1) by basing ourselves firstly upon facts which have been stated quite reliably at the moment.

Schottky solution. At first let us analyze the solutions of equation (2.1) for the case when the coefficients of that equation are constant over the discharge tube cross-section. This occurs at relatively low input energies, which leave the spatial temperature uniformity in the plasma volume undisturbed. It should be noted that in this case taking account of the electron attachment to neutrals does not change the form of equation, but only requires a change of the coefficient ν_{ion} for the corresponding effective quantity equal to the difference: $\nu_{eff} = \nu_{ion} - \gamma N$. Obviously, the stationary discharge is feasible only if this difference is positive. The simplest case (Schottky solution) in respect to analysis corresponds to the situation where the volume recombination of charged particles in plasma is negligible, and the diffusion removal to the walls proceeds as the main mechanism of their neutralization. In this case, which takes place at moderate currents and relatively low pressures, the solution of equation (2.1) has the following form [12]:

$$N_e(r) = N_e(0) J_0\left(\frac{\beta r}{R_0}\right) , \quad (2.4)$$

where $J_0(x)$ is the zero-order Bessel function and $\beta = 2.405$ in accordance with the boundary condition (2.2). The same condition provides the interrelationship between the coefficients of equation (2.1):

$$\frac{\nu_{eff} R_0^2}{D_a} = \beta^2 \equiv 5.77 , \quad (2.5)$$

which in its turn determines the dependence of the reduced electrical field strength E/N on the product NR_0.

The last relationship reflects the balance of charged particles, which are generated in the discharge bulk and neutralized on the walls as a result of ambipolar diffusion. Independently on the character of approximations used in the analysis of equation (2.1), its solution has to be supplemented with the balance relationship which is similar to (2.5). This latter states the interconnection between discharge parameters. The situation involved is typical of transfer equations with zero boundary conditions.

Considering the volume recombination. Let us take into consideration a possibility of the volume recombination of charged particles. Setting for simplicity sake $N_e = N_i$, we can conclude that the volume recombination, which is proportional to the square of the electron number density, makes the most significant contribution to the central, near-axis region of a discharge tube, where the electron number density is maximal [13]. In this region, the radial decrease in the electron number density appears to be smoother than in the absence of the volume recombination. For comparison of electron number density radial dependencies in the presence and

absence of the recombination near the discharge tube walls, it is convenient to multiply equation (2.1) written in a cylindrical frame of reference, by rdr and to integrate it over all the cross-section of the discharge tube from 0 to R_0. This results in

$$\nu_{\text{ion}} \int n_{\text{e}}(r)\, r\, \mathrm{d}r = \alpha_{\text{rec}} N_{\text{e}}(0) \int n_{\text{e}}^2(r)\, r\, \mathrm{d}r - D_{\text{a}} R_0 \frac{\mathrm{d}n_{\text{e}}}{\mathrm{d}r}\,(r = R_0)\,. \tag{2.6}$$

Here $n_{\text{e}} = N_{\text{e}}/N_{\text{e}}(0)$ is the dimensionless electron number density. It could be noted that the last term in the right side of (2.6) is negative, so the recombination and diffusion contributions are added. The expression in the left side of (2.6) is proportional to the net discharge current. As it follows from equation (2.6), when the discharge current is steady, an increase in the recombination loss is accompanied by a lowering in the relative contribution of the last term in (2.6), i.e. lowering in the derivative of the electron number density near the wall. Comparing this solution with the Schottky solution (2.4), it might be inferred that the inclusion of recombination makes the radial distribution of electron number density to be radially decreasing more smoothly in the near-axis region and decreasing more drastically close to the tube wall. The solutions of equation (2.1) with and without allowance made for the volume recombination are depicted in Fig. 1 (curves *a* and *b*, correspondingly).

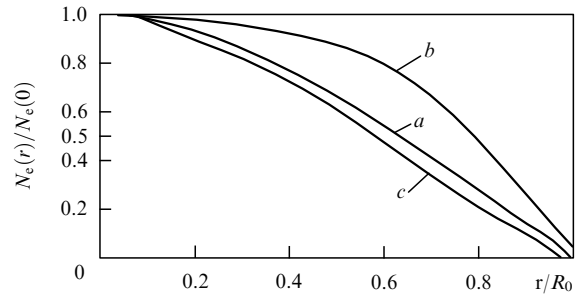

Figure 1. Radial dependencies of charged particles number density as stated on the basis of solution to Eqn (2.1) without (*a*) and with allowance (*b*, *c*) made for volume recombination. Curve *c* is related to the condition $\alpha_{\text{rec}} N_{\text{e}}(0) R_0^2/6D_{\text{a}} = 10$. All curves are normalized to the same axial electron number densities.

Nonuniform ionization. As may be seen from the analysis performed above, the spatial electron number density distribution constituting the solution of the balance equation (2.1) with radially constant coefficients, is a smooth radially decreasing function. The discharge fills essentially the whole volume of a tube and does not experience constriction. Let us consider a change in the character of solution to equation (2.1) resulting from taking into account the radial dependencies of its coefficients. As it will be seen from the subsequent analysis, the most drastic radial dependence is usually inherent in the rate constant of atomic or molecular ionization with an electron impact. The situation is conditioned by the dependence of that parameter on both the E/N ratio and ionization degree of plasma. Let us analyze the balance equation (2.1) for electron number density by taking account of the abrupt radial dependence of the parameter ν_{eff}. At first the charged particle volume recombination is supposed to be ignored. The real radial dependence of the parameter ν_{eff} will be replaced with the model one by presetting the size r_0 of the region in which the effective formation of charged particles takes place:

$$\nu_{\text{eff}}(r \leqslant r_0) = \nu_0; \qquad \nu_{\text{eff}}(r > r_0) = 0\,. \tag{2.7}$$

Multiplying relation (2.1) by $r\,\mathrm{d}r$ and integrating it from 0 to R_0 with due regard for (2.7), as well as ignoring the volume charged particles recombination will result in

$$\frac{\mathrm{d}N_{\text{e}}}{\mathrm{d}r}\,(R_0) = \frac{\nu_0}{D_{\text{a}} R_0} \int_0^{r_0} N_{\text{e}}(r)\, r\, \mathrm{d}r\,. \tag{2.8}$$

The right side of the relationship obtained is proportional to the number of charged particles formed in a unit time per unit length of a plasma column. The magnitude of this parameter is determined by the value of the net discharge current and is rather weakly sensitive to the size of the region where the charged particles are generated. Hence, in the absence of the charge particles volume recombination, the derivative of the electron number density $\mathrm{d}N_{\text{e}}(R_0)/\mathrm{d}r$ is not small as it would be in the case of constriction. Thus, in the absence of recombination even a sharp spatial nonuniformity in the ionization rate constant does not cause constriction.

The form of the solution to equation (2.1) changes in a qualitative manner in the case that, on the one hand, the rate of charged particles generation is a drastically decreasing radial function and, on the other hand, the charged particles neutralization is mainly resulted from the volumetric processes. The last condition takes the following form:

$$\frac{6D_{\text{a}}}{R_0^2} \ll \alpha_{\text{rec}} N_{\text{e}}^0\,, \tag{2.9}$$

where N_{e}^0 is the characteristic magnitude of the electron number density in a discharge tube. This condition is valid at relatively high currents and pressures. In the limiting case of very high pressures where diffusion is negligible, equation (2.9) results in

$$N_{\text{e}}(r) = \frac{\nu_{\text{eff}}(r)}{\alpha_{\text{rec}}}\,. \tag{2.10}$$

The recombination coefficient is usually much less radial-dependent function in comparison with the ionization rate constant. For this reason, in absence of diffusion, the radial dependence of the electron number density is practically close to that of the function $\nu_{\text{eff}}(r)$. Physical reasons determining rather drastic behaviour of this dependence will be considered below.

Radius of the constricted column. It should be emphasized that solution (2.10) obtained above does not obey boundary condition (2.2). This contradiction is formal in the case where the ionization rate constant decreases quite sharply in radial direction and the electron number density near the wall is negligible. However, a radial decrease in the electron number density is followed by a rise in the characteristic time $\tau_{\text{rec}} \sim (\alpha_{\text{rec}} N_{\text{e}})^{-1}$ for the charged particles recombination. In its turn this causes the violation of above-accepted condition (2.9) concerning the neglecting role of diffusion. However, allowance made for diffusion is necessary for both the proper estimation of the transverse size of the constricted discharge and correct determination of the radial decrease in the electron number density near the wall. Thus, if free electrons are formed mainly within a narrow near-axis region of the discharge tube, the characteristic radius r_{c} of a region filled with the constricted discharge can be estimated as the

distance passed by an electron in the course of ambipolar diffusion in the recombination time:

$$r_c \sim \sqrt{D_a \tau_{rec}} \sim \sqrt{\frac{D_a}{\alpha_{rec} N_e^0}} . \quad (2.11)$$

It is easy to verify that on meeting condition (2.9) the radius of the region filled with discharge is much less than that of a discharge tube. Thus the mechanism for the discharge constriction becomes clear. Under conditions of a spatially nonuniform gas discharge plasma, the free electrons are formed mainly in the narrow axial region of a discharge tube. On satisfying condition (2.9) the major portion of charged particles is neutralized in the plasma volume and has no time to reach the wall. So the radius of the region filled with discharge turns out to be much less than the radius of a discharge tube. Estimating the radius of the region filled with charge particles for a specific physical situation it is necessary to take into account a finite size of the region wherein their generation proceeds. In view of that the magnitude of r_c has to exceed somewhat estimation (2.11).

It should be emphasized that the exact analytical solution of the electron number density balance equation is attainable only for the Schottky limiting case considered above. Generally speaking this nonlinear equation is not soluble analytically even though its coefficients are constant. Thus, the determination of the charge particles radial distribution is based usually on numerical methods. One of those methods which manifested itself quite well in practice [9, 11] merits a special attention. This approximate method for solution of equation (2.1) is based on representation of the function under investigation in terms of varying parameters C and α which determine the absolute magnitude of the electron number density in a discharge and a degree of steepness of its radial decrease. In accordance with that method, the solution of equation (2.1) is expressed in the simple approximate form:

$$N_e(\rho) = C\left[\exp(-\alpha\rho^2) - \exp(-\alpha)\right] . \quad (2.12)$$

Here $\rho = r/R_0$ is the dimensionless radial coordinate. Trial function (2.12) obeys boundary conditions (2.2), (2.3) automatically. This permits us to represent in a unified manner both the diffusive (at $\alpha \leqslant 1$) and constricted (at $\alpha \gg 1$) radial distributions of charged particles. The magnitudes of the varied parameters α and C are determined as a result of solution of two transcendental equations. The first of these equations is the result of substitution of expression (2.11) into equation (2.1) and its subsequent integration with respect to $r\,dr$ from 0 to R_0. The second one is the result of substitution of the same expression into equation (2.1) and its solution at $r = 0$.

Some notion about the accuracy of the method considered can be obtained by comparing the approximate solution of equation (2.1) in the case of constant coefficients and without regard for the volume recombination (Schottky case) with the exact solution (2.4). Performing the procedures indicated above results in the following set of equations:

$$\frac{4D_a\alpha}{R_0^2} = \nu_{eff}\left[1 - \exp(-\alpha)\right] , \quad (2.13)$$

$$\frac{4D_a\alpha\,\exp(-\alpha)}{R_0^2} = \nu_{eff}\left[\frac{1-\exp(-\alpha)}{\alpha} - \exp(-\alpha)\right] . \quad (2.14)$$

Due to a linear form of the initial equation, the result of calculation does not contain the quantity C. The set of transcendent equations (2.13), (2.14) is solved quite easily with a calculator:

$$\alpha = 0.842;$$

$$\nu_{eff}\frac{R_0^2}{D_a} = \frac{4\alpha}{1-\exp(-\alpha)} = 5.9 . \quad (2.15)$$

The solution obtained coincides very closely with the exact result (2.4). It can be verified quite easily by calculating the following integral:

$$I = \int_0^1 \left\{ C\left[\exp(-\alpha\rho^2) - \exp(-\alpha)\right] - J_0(2.405\rho) \right\}^2 \rho\,d\rho ,$$

where the parameter C is determined through the normalization expression for the electron number density radial distribution:

$$C\int_0^1 \left[\exp(-\alpha\rho^2) - \exp(-\alpha)\right]\rho\,d\rho = \int_0^1 J_0(2.405\rho)\rho\,d\rho .$$

The calculations result in $I = 2.26 \times 10^{-7}$, i.e the approximate solution agrees very closely with the exact one. The described above simple approximate method of the solution of the electron number density balance equation (2.1) is used quite successfully when solving this equation in much more complicated situations [11], which require taking into consideration both the volume recombination and spatial nonuniformity of the coefficients of equation (2.1).

2.3 Constricted discharge in the presence of electron attachment

The role of electron attachment to neutrals in the formation of the charged particles spatial distribution is similar to that of above-considered volume recombination. Thus, in the case where the rate constant of charged particles formation decreases drastically from the axis to the wall of a discharge tube, whereas the characteristic time of electron attachment $\tau_{at} \sim 1/\gamma N$ is much less than that for diffusive removal of charged particles to the discharge tube wall $\tau_{dif} \sim R_0^2/6D_a$, viz.

$$\frac{1}{\gamma N} \gg \frac{R_0^2}{6D_a} , \quad (2.16)$$

the discharge becomes constricted [14, 15]. However, diffusion of charged particles always plays a considerable role in their balance and has to be considered under the analysis of the radial distribution. Thus, if the size of the region of predominant ionization r_i is much less than the tube radius R_0, then the charged particles radial distribution in the major region of a discharge tube, where ionization is negligible, is resulted from the equation

$$\frac{1}{r}\frac{d}{dr}\left(rD_a\frac{dN_e}{dr}\right) - \gamma N N_e = 0 \quad (2.17)$$

with boundary conditions $N_e(0) = N_0$, $N_e(R_0) = 0$. The solution of that equation for the main region

$$\left(\frac{D_a}{R_0^2\gamma N}\right)^{1/2} R_0 \ll r < R_0$$

takes the following form:

$$N_e(r) \approx N_0 \left\{ \exp\left[-\left(\frac{\gamma N}{D_a}\right)^{1/2} r \right] - \exp\left[-\left(\frac{\gamma N}{D_a}\right)^{1/2} R_0 \right] \right\}. \tag{2.18}$$

As seen from this solution, the characteristic size of a region filled with electrons $r_e \sim (D_a/\gamma N)^{1/2}$ may be considered as the distance passed by the diffusing particle in the attachment time $1/\gamma N$. The analysis of charged particles balance equation given above shows that the constricted distribution of charged particles over the discharge tube cross-section is realized under conditions when the charged particles formation proceeds in a narrow near-axis region of a tube and their volume neutralization prevails over diffusive removal to the wall. The specific physical situations wherein the indicated conditions are satisfied will be treated below.

2.4 Thermally nonuniform plasma

The thermal nonuniformity of a gas discharge gives the most general cause for its spatial nonuniformity. A sizable part of the input energy is removed to the tube wall as a result of the molecular heat conductivity. This causes a difference in temperature between the axis and the wall of a discharge tube, the magnitude of which rises as the input energy increases. Since the gas pressure p is constant over the cross-section of a discharge tube, the spatial nonuniformity in temperature causes analogous nonuniformity in the reduced electrical field strength E/N by virtue of the gas state equation $p = NT$. In its turn, this results in a drastic radial dependence of the rate constant for ionization of atoms or molecules by electron impact. It is convenient to express the degree of steepness of that dependence through its logarithmic derivative

$$b_i = \left.\frac{\mathrm{d}\ln \nu_{ion}}{\mathrm{d}\ln T}\right|_{p=\mathrm{const}} = \frac{\mathrm{d}\ln \nu_{ion}}{\mathrm{d}\ln(E/N)}. \tag{2.19}$$

In conditions relevant to a weakly ionized plasma, where electron-electron collisions have little or no effect on the electron energy distribution function, the magnitude of the parameter b_i is determined by the ratio E/N and does not depend on ionization degree of plasma. The magnitudes of that parameter determined on the base of experimental dependencies $\nu_{ion}(E/N)$ are compiled in Table 1. As seen, these magnitudes are in excess of unity over a wide range of discharge parameters. It means that a relatively low difference in temperature (of the order of temperature itself) can cause a difference in the ionization rate constant as high as several orders of magnitude.

Table 1. Values of b_i versus ratio E/N for the discharge initiated in some gases [16].

Gas	Values of b_i at E/N, 10^{-16} V cm^2 equal to						
	0.5	1	3	5	10	30	40
He	—	—	2.8	3.3	1.3	0.84	—
Ne	3.1	3.1	2.4	2.1	1.3	1.0	0.5
Ar	—	—	4	3.2	2.6	1.9	0.85
Kr	—	—	4	3.2	2.6	1.9	0.85
Xe	—	—	6	4.6	3.0	2.1	1.2
H_2	—	—	—	10	3.3	1.3	0.54
D_2	—	—	—	8	2.9	1.3	0.5
O_2	—	—	7.7	4.6	3.0	—	—
CO	—	—	—	—	—	3.9	1.3
N_2	—	—	—	10.4	5	2.3	0.85
CO_2	—	—	2	0.6	0.9	1.4	1.0

2.5 Recombination mechanism for disconstriction of a discharge

A predominance of volume charged particles recombination over surface one is a necessary condition for the constriction of a discharge column. Among various mechanisms of volume recombination which can be realized in a gas discharge plasma, the dissociative recombination of electrons and molecular ions

$$e + AB^+ \Rightarrow A + B \tag{2.20}$$

occupies a prominent place [17–19]. As a result of this process one of the atoms (A or B) can be found in an excited state. The energy released in the course of formation of the electron bound state is transformed into the kinetic energy of atoms flying apart. For this reason, process (2.20), which does not require the third particle participation, is characterized by a quite high intensity in conditions pertaining to a gas discharge plasma with molecular ions. The typical value of a rate constant of the process under consideration at $T_e \approx 1-3$ eV lies in the range $10^{-8}-10^{-7}$ cm^3 s^{-1}, whereas that for the triple recombination process

$$2e + A^+ \Rightarrow A + e \tag{2.21}$$

is as low as 7–8 orders of magnitude in the similar conditions and $N_e \approx 10^{12}$ cm^{-3}. It follows that the volumetric mechanism for charged particles neutralization predominates over the surface one only if a plasma contains molecular ions.

In a molecular gas discharge where molecular ions usually belong to the prevailing sort of ions, the dissociative recombination is the main channel for the volume neutralization of charged particles. In a rare-gas discharge, molecular ions predominate over atomic ones at relatively high pressures and moderate gas temperatures. Estimation of the relative content of atomic N_{1i} and molecular N_{2i} ions in a rare-gas discharge can be performed on the base of the equilibrium relationship

$$\frac{N_{1i}N}{N_{2i}} = \frac{g_{1i}g_a}{g_{mol}} \exp\left(-\frac{D}{T}\right) \frac{1}{2\pi r_0^2} \sqrt{\frac{\mu T}{2\pi\hbar}} \left[1 - \exp\left(-\frac{\hbar\omega}{T}\right)\right], \tag{2.22}$$

where g_a, g_{1i}, g_{mol} are the statistical weights of corresponding neutral and ionized particles; r_0 is the equilibrium internuclear distance; μ, reduced mass; D, dissociation energy, and $\hbar\omega$ is the vibrational energy quantum for the molecular ion.

The dissociation energies of rare-gas molecular ions lie in the range 1–2 eV, therefore, as it follows from expression (2.22), the molecular ions prevail over the atomic ones only at moderate gas temperatures $T \leqslant 1000$ K. The inert gas temperatures at which the equilibrium values of atomic and molecular number densities (calculated on the base of relation (2.22)) were equal to each other are presented in Table 2. Of course, these values depend on the number density of neutral atoms.

The temperature dependence of the relative content of molecular ions in a rare-gas discharge forms the basis of a noteworthy mechanism for its disconstriction at elevated

Table 2. Inert gas temperatures (K), at which the equilibrium number densities of atomic and molecular ions become equal [9].

N, cm^{-3}	Gas temperature, K				
	He	Ne	Ar	Kr	Xe
10^{16}	1530	740	910	780	650
10^{17}	1740	870	1060	900	740
10^{17}	2100	1010	1250	1050	860
10^{18}	2630	1230	1500	1250	1010

input energies. This phenomenon has been observed by V Baranov and K Ul'yanov [20] and described theoretically in works [21, 22] after a while. In accordance with this mechanism, at a moderate energy input when the gas temperature in the axial region of a discharge tube does not exceed values given in Table 2, the molecular ions prevail thus promoting the discharge constriction. Further increase in the energy input gives rise to the gas temperature at a time. This brings about the thermal destruction of molecular ions and as a consequence a decline in the contribution of the volume neutralization to the charged particles balance. In its turn this is accompanied by upsetting of the gas discharge constriction and, correspondingly, by a rise in the cross-section of the area filled with the discharge current. A rough estimation of the constricted discharge radius may be performed in this case on the base of the solution to the heat conduction equation, namely, considering this value as a dimension of the region where the gas temperature is so high that the relative content of molecular ions is negligible [21]. A rise in the input energy is followed by that in the size of the region filled with a discharge. This is just an essence of the disconstriction phenomenon. The latter is illustrated in Fig. 2 where dependence of the relative radius of the constricted discharge in Ar on the current measured at various gas pressures is given [20].

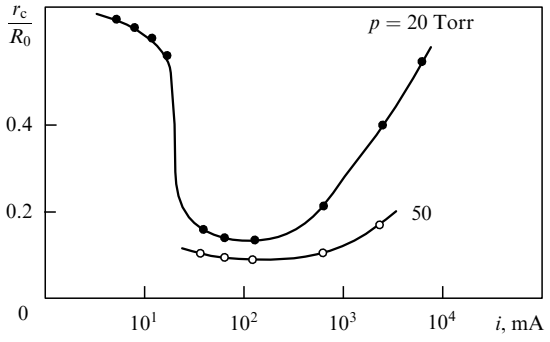

Figure 2. The dimensionless constriction radius r_c/R_0 versus the discharge current measured at different pressures and $R_0 = 1.3$ cm [20].

2.6 Constriction of a molecular gas discharge

The main distinctive feature of a molecular gas discharge results from the existence of inner molecular degrees of freedom which are related to their vibrational and rotational motions. As it follows from the results of a number of experimental and theoretical studies [23–24], the main portion (usually over 90%) of energy input to a molecular gas discharge therewith is expended for the excitation of molecular vibrations. The vibrational energy is further transformed into translational one as a result of intermolecular collisional relaxation. However, the rate of this transformation is rather small. For instance, transformation of a quantum of vibrational energy of N_2 molecule into thermal energy at room temperature requires more than 10^{10} intermolecular collisions. For this reason, over a wide range of discharge parameters the state of a molecular gas is far from equilibrium. This state is characterized by an extraequilibrium vibrational energy content. The transformation of this inner energy into that of translational motion, i.e. into heat, proceeds extremely slowly, so the main portion of the vibrational energy of molecules is removed to the wall as a result of diffusion, whereas the translational gas temperature remains to be relatively small.

The rise in the energy input and/or gas pressure causes an increase in importance of volumetric vibrational relaxation processes and their contribution to the balance of molecular vibrational energy. This is accompanied also by an enhancement in the translational gas temperature and, as a consequence, in the spatial nonuniformity of a gas discharge column. The transition of a molecular gas discharge from the mode with diffusive removal of vibrational energy to the walls to that with volumetric vibrational relaxation can proceed in an avalanche-like, explosive manner [25–27]. This results from the strong temperature dependence of the vibrational relaxation rate constant. Local gas heating due to possible current fluctuations is accompanied by a drastic rise in the vibrational relaxation rate constant of molecules, which in turn stimulates further gas heating. If the time required for smoothing (through molecular heat conduction) the formed local thermal nonuniformity exceeds the characteristic time of the vibrational relaxation at local magnitude of gas temperature, the avalanche-like rise in gas temperature takes place, which is accompanied by the change in the prevailing mechanism of vibrational relaxation. As a result of this temperature rise, which is similar to a thermal explosion, a gas discharge column becomes to be spatially nonuniform, whereas a molecular gas changes to the state close to thermodynamically equilibrium one.

The analysis of conditions governing the transition of a molecular gas discharge from the mode with diffusive removal of vibrational energy to the walls to that with volumetric vibrational relaxation will be performed on the base of a simple model [25] involving the balance equations for translational and vibrational energies. The mean number of vibrational quanta per molecule is denoted in what follows by ε. Assuming that the vibrationally excited molecules are formed as a result of electron-molecule collisions (rate constant of this process is k_{eV}) and removed to the walls through diffusion (characteristic time is τ_D), one obtains the steady-state balance equation for the vibrational energy:

$$\frac{\varepsilon - \varepsilon_0}{\tau_D} = N_e N k_{eV} . \tag{2.23}$$

This equation has to be analyzed in combination with the heat conduction equation, a simplified form of which looks as

$$C_V \frac{T - T_0}{\tau_T} = \frac{\varepsilon - \varepsilon_0}{\tau_{VT}} \hbar\omega . \tag{2.24}$$

Here C_V is the specific heat capacity of a gas at a constant pressure, τ_T is the characteristic time for heat conductivity, $\hbar\omega$ is the energy of vibrational quantum of a molecule, τ_{VT} is the

characteristic time of collisional vibrational relaxation; subscript 'zero' denotes the equilibrium values of parameters ε and T which are reached at the discharge tube wall. It is presumed therewith that while the portion of vibrational energy released in a volume as a heat is relatively low, just this process provides the main source of gas heating. Such an assumption is justified over a wide range of discharge parameters because in a molecular gas discharge the contribution of other sources of heating (elastic electron-molecule scattering, excitation of molecular rotation) is usually still lesser. Inserting the dimensionless temperature

$$\Theta = \frac{T - T_0}{T_0} \tag{2.25}$$

and approximating the abrupt temperature dependence of the molecular vibrational relaxation rate to the standard exponential form [28]

$$\frac{1}{\tau_{VT}} = \frac{1}{\tau_{VT}(T_0)} \exp(b_{VT}\,\Theta)\,, \tag{2.26}$$

the set of equations (2.23), (2.24) can be brought to the form

$$\Theta = A \exp(b_{VT}\,\Theta)\,. \tag{2.27}$$

Here the factor

$$A = \frac{N_e N k_{eV}\,\hbar\omega\,\tau_T\,\tau_D}{C_V \tau_{VT}(T_0)\,T_0}\,, \tag{2.28}$$

and parameter

$$b_{VT} = \frac{\mathrm{d}\ln(1/\tau_{VT})}{\mathrm{d}\ln T}\,(T = T_0) \gg 1 \tag{2.29}$$

determines a degree of steepness for the temperature dependence of molecular vibrational relaxation rate. In Table 3, the values of this parameter are given and they were determined on the base of measurements at various temperatures [16]. As is seen, the condition $b_{VT} \gg 1$ which provides the basis for expansion (2.26) is obeyed quite well at moderate temperatures.

Table 3. Values of the parameter b_{VT} defined by expression (2.29) as determined from measurements of $k_{VT}(T)$ for various gases.

T, K	Values of b_{VT} for various gases					
	H_2	D_2	N_2	O_2	CO	Cl_2
200	3.2	3.2	3.4	2.9	2.4	1.6
300	4.2	6.3	10.7	4.5	5.5	2.8
500	3.7	4.8	14.2	7.0	6.7	3.8

Equation (2.27) is well known in chemical physics, because it determines the thermal explosion condition for an exothermic chemical reaction [28]. It is easily seen that the steady-state solution of this equation exists only at the condition

$$A \leqslant \frac{1}{b_{VT}\,\mathrm{e}} \tag{2.30}$$

(e is the base of the natural logarithm). If condition (2.30) is obeyed, equation (2.27) has two solutions, one of which (low-temperature) is stable, whereas the high-temperature one is unstable with respect to temperature fluctuations. The inequality which is opposite to (2.30) constitutes the condition for the thermal instability of a molecular gas discharge. This condition is fulfilled on exceeding certain value of the discharge current or gas pressure.

2.7 Nonthermal mechanism of gas discharge constriction

One more physical mechanism defining the possibility of disturbance of the spatial uniformity in gas discharge parameters, relates to the dependence of the electron energy distribution function on the ionization degree of a gas discharge plasma [29 – 32]. Such a dependence is typical for an inert gas discharge and can be realized in conditions where the electron-electron and elastic electron-atom collisions make comparable contributions to the electron energy balance.

The range of plasma parameters, wherein a drastic dependence of the gas particles ionization rate constant on the ionization degree occurs, can be estimated in the following way. In two limiting cases, the electron energy distribution function does not depend on the electron number density. Namely, at low ionization degrees, where the relationship

$$\nu_{ee} \ll \frac{m}{M}\,\nu_{ea} \tag{2.31}$$

is valid at any electron energy (m, M are the electron and atomic mass, correspondingly, ν_{ee}, ν_{ea} are the rate constants for the electron-electron and elastic electron-atom collisions, respectively), the electron energy distribution function $f(\varepsilon)$ is determined mainly by the electron-atom collisions and can be expressed in the form [33]:

$$f(\varepsilon) = C \exp\left[-\int_0^{\varepsilon} \frac{\mathrm{d}\varepsilon}{T + e^2E^2M/(3m^2\nu_{ea}^2)}\right]. \tag{2.32}$$

In the opposite limiting case, where the relationship takes place in the form

$$\nu_{ee} \gg \frac{m}{M}\,\nu_{ea}\,, \tag{2.33}$$

the electron energy distribution function has the Maxwellian form

$$f(\varepsilon) = \frac{2}{\sqrt{\pi}}\,T_e^{-3/2} \exp\left(-\frac{\varepsilon}{T}\right)\sqrt{\varepsilon}\,. \tag{2.34}$$

In the range of the plasma ionization degrees which is intermediate between ranges (2.31) and (2.33), the electron energy distribution function depends on the ionization degree of plasma. In contrast to the electron-atom elastic collision rate ν_{ea}, the electron-electron collision rate

$$\nu_{ee} = \frac{2\pi e^4}{\varepsilon^2}\,N_e\sqrt{\frac{2\varepsilon}{m}}\,\ln\Lambda \tag{2.35}$$

($\ln\Lambda$ is the Coulomb logarithm) is characterized by the sharply falling energy dependence. For this reason, the situation is typical where in the low electron energy range inequality (2.33) is valid, and the electron energy distribution function has the near-Maxwellian form, whereas in the electron energy range close to the atomic-resonance excitation threshold the opposite relation (2.31) is valid. In this range, equation (2.32) is more proper for description of the

electron energy distribution function. This equation provides a sharper fall of the function with increase in electron energy.

The region of intermediate electron energies, where the electron energy distribution function undergoes transition from the Maxwellian form (2.34) to function (2.32), is determined by the ionization degree of plasma. For this reason, the values of rate constants for both the excitation of atomic resonance states and ionization of an atom by an electron impact are sharply increasing functions of the ionization degree of a plasma. The form of those functions can be determined on the base of solution to the Boltzmann kinetic equation with consideration for both the interelectron and electron-atom collisions. Approximate methods of the solution to this nonlinear integral equation were developed in Refs [34–37], where the rate constants of atomic ionization by an electron impact were calculated as a function of the ionization degree of a rare-gas plasma. The authors treated the case where the main mechanism of charged particles formation relates to the step atomic ionization.

The sharp increasing fashion of the dependence involved in the case of a volume neutralization of charged particles causes the discharge constriction even in the absence of a thermal nonuniformity, i.e. at relatively low input energies. This nonthermal mechanism of a gas discharge spatial nonuniformity is realized in a region of moderate ionization degrees of plasma:

$$\frac{1}{2\pi}\frac{m}{M}\frac{\sigma_{ea}(T_e)\,T_e^2}{e^4\ln\Lambda} \leqslant \frac{N_e}{N} < \frac{1}{2\pi}\frac{m}{M}\frac{\sigma_{ea}(I_t)\,I_t^2}{e^4\ln\Lambda}\,. \tag{2.36}$$

Here σ_{ea} is the cross-section of elastic electron-atom collisions, e is the electron charge, T_e is the electron temperature, I_t is the energy of a resonance atomic level, $\ln\Lambda \approx 10$ is the Coulomb logarithm. At values of $T_e \approx 1$ eV, $I_t \approx 15$ eV, $\sigma_{ea}(T_e) \approx \sigma_{ea}(I_t) \approx 10^{-15}$ cm^{-2}, which are typical for a rare-gas discharge plasma, condition (2.36) relates to the region of a plasma ionization degree $N_e/N \approx 10^{-6}-10^{-4}$.

3. Thermal regime of a gas discharge plasma

3.1 Local thermodynamic and ionization equilibrium

Let us consider a state of a gas discharge plasma which is realized in a high-pressure arc discharge and is spoken of as local thermodynamic equilibrium. Due to a high number density of atoms and a high number density of electrons, collisional processes in this state are more essential than transport ones. Hence, transport of particles owing to nonuniformity of plasma is not essential, and a near-equilibrium state is supported at each plasma point which is characterized by certain gaseous T and electron T_e temperatures, and corresponds to the Maxwellian distribution functions of electrons and atoms over velocities.

These temperatures are established due to processes of electron interaction with external fields, collisional processes with electrons and atoms, and heat transfer lengthwise of the discharge tube cross-section. But the relation between electron and gaseous temperatures is determined by collisional processes and interaction of electrons with external fields alone, so that transport processes leave this relation unaffected. In particular, if a gas-discharge plasma is supported by a constant electric field of the strength E, then the difference of the electron and gaseous temperatures is equal to

$$T_e - T = \frac{Ma^2}{3}\frac{\langle v^2/\nu\rangle}{\langle v^2\nu\rangle}\,, \tag{3.1}$$

where M is the atomic mass, $a = eE/m$, e is the electron charge, angular brackets stand for averaging of the corresponding quantity over electron velocities v with the Maxwellian distribution function, ν is the electron-atom collision frequency. Specifically, if the collisional frequency does not depend on the electron velocity, formula (3.1) has the form [33, 38, 39]:

$$T_e - T = \frac{Mw^2}{3}\,, \tag{3.2}$$

where w is the electron drift velocity.

Local thermodynamic equilibrium is attained in a gas-discharge plasma if a time of energy exchange between electrons as a result of their collisions proves to be small in comparison to that of energy exchange with atoms and also to typical times of the electron energy transport to other discharge regions; the same criterion must be satisfied for atoms. We shall consider below the regime of local ionization equilibrium which requires a more rigorous criterion. In this regime, the electron number density N_e at each point of a gas-discharge plasma is connected with the atomic number density N by the Saha formula [33]

$$\frac{N_e^2}{N} = \frac{g_e g_i}{g_a}\left(\frac{mT_e}{2\pi\hbar^2}\right)^{3/2}\exp\left(-\frac{J}{T_e}\right). \tag{3.3}$$

For simplicity, we consider only one-component atomic gas. Here J is the atomic ionization potential, m is the electron mass, $\hbar$ is the reduced Plank constant, $g_e = 2$, g_i, g_a are the statistical weights of an electron, ion and atom, respectively. Notice that because of the condition $T_e \ll J$ (in this paper we express temperatures in energetic units) the number density of excited atoms is small compared to that for atoms in the ground state, so that excited atoms do not make a contribution to the total atomic number density. Furthermore, the gas-discharge plasma considered is quasi-neutral: $N_e = N_i$. The criterion of the validity of the local ionization equilibrium takes the form

$$\tau_{rec} \ll \tau_{dif}\,, \tag{3.4}$$

where $\tau_{rec} \propto (KN_e^2)^{-1}$ is the typical time of recombination for a probe electron, $\tau_{dif} = R_0^2/5.78D_a$) is a typical time of electron drift from the plasma-filled region. Here K is the rate constant of three-body recombination of electrons and ions which is given by the formula [18]

$$K = 6.4\times10^{-22}\,\mathrm{cm^6\,s^{-1}}\left(\frac{1000}{T_e}\right)^{9/2},$$

where the electron temperature T_e is expressed in kelvin, R_0 is a plasma radius, D_a is the coefficient of ambipolar diffusion which is expressed through the ion diffusion coefficient by the formula

$$D_a = D_i\left(1+\frac{T_e}{T}\right).$$

Thus, the criterion of local ionization equilibrium is satisfied if the parameter

$$\eta = \frac{\tau_{dif}}{\tau_{rec}} = \frac{KN_e^2R_0^2}{5.8D_a} \tag{3.5}$$

is large. Further we will check the validity of this criterion for a certain gas-discharge plasma under consideration.

3.2 Heat balance of a gas-discharge positive column

Let us consider the heat balance of the positive column of gas discharge assuming the heat removal to be determined by thermal conductivity. Then the heat balance equation has the following form for a cylinder discharge tube:

$$\frac{1}{r}\frac{\mathrm{d}}{\mathrm{d}r}\left(\varkappa(T)r\frac{\mathrm{d}T}{\mathrm{d}r}\right)+p(r)=0\,, \tag{3.6}$$

where $\varkappa(T)$ is the heat conduction coefficient, $p(r)=iE$ is the specific power of heat release, so that i is the electric current density, E is the longitudinal electric field strength in the discharge.

Equation (3.6) permits the temperature difference between the axis and walls in a gas-discharge tube to be determined. Assume that the radial distribution of the electron number density is governed by the Schottky expression (2.4), which corresponds to the case where the heat release caused by the electric current flow through a gas does not affect the electron density radial distribution. As this takes place, the last term in equation (3.6) has the form

$$p(r)=p_0J_0\left(\frac{2.4r}{R_0}\right).$$

Let us approximate the temperature dependence of the heat conduction coefficient with the power function

$$\chi(T)=\chi_0\left(\frac{T}{T_0}\right)^n,$$

where T_0 is the near-wall gas temperature. Thus we obtain the following equation:

$$\frac{\chi_0}{(n+1)}\frac{1}{r}\frac{\partial}{\partial r}\left(r\frac{\partial}{\partial r}T^{n+1}\right)=-p_0T_0^nJ\left(2.4\frac{r}{R_0}\right). \tag{3.7}$$

Double integration of this equation with due regard for the boundary conditions formulated above results in

$$T(r)=T_0\left[1+\frac{0.13(n+1)P_lJ_0(2.4r/R_0)}{\chi_0T_0}\right]^{1/(n+1)}, \tag{3.8}$$

where $P_l=iE=1.36p_0R_0^2$ is the power released per unit length of a discharge tube. This expression is valid on condition that the emission of light takes away relatively small portion of the input energy.

From expression (3.8) it follows the relationship for the temperature difference between the axis and wall:

$$T(0)-T_0=T_0\left[1+\frac{0.13(n+1)P_l}{\chi_0T_0}\right]^{1/(n+1)}. \tag{3.9}$$

For the majority of gases the parameter n is close to or somewhat below unity, so the temperature difference in a discharge tube may be thought of as proportional to the square root of the total power input to a good approximation.

Let us consider this problem more generally. The distribution of the specific power of heat release over the tube cross-section may be specified in the form

$$p=p_0\left[1-\left(\frac{r}{R_0}\right)^{\alpha}\right].$$

Then the power of heat release per unit length of the discharge tube is equal to

$$P=\pi p_0\frac{R_0^2\alpha}{\alpha+2}\,,$$

whereas the temperature difference can be expressed through equation (3.9) with the numerical coefficient dependent on the parameter α:

$$T(0)-T_0=T_0\left[1+\frac{f(\alpha)(n+1)P_l}{\chi_0T_0}\right]^{1/(n+1)}, \tag{3.9a}$$

here $f(\alpha)=(\alpha+4)/4\pi(\alpha+2)$. As is easy to see, the temperature difference in a discharge is only weakly sensitive to the radial distribution of the thermal sources. Thus, at $(n+1)P_l/\chi_0T_0=1$, the variation of the parameter α from 1 up to 10 tends to lower the relative temperature difference by 1.5%, whereas at $(n+1)P_l/\chi_0T_0=10$ such a decrease does not exceed 8%. In this manner the specific power input P_l uniquely determines for all practical purposes both the difference and the radial distribution of temperature in a discharge.

Relationship (3.9) is convenient for the analysis of the thermal regime of a glow discharge. Let us demonstrate it by the example of a gas-discharge CO_2-laser. Its radiation power increases with a rise in the discharge power. But processes of vibrational relaxation, which correspond to quenching of vibrationally excited molecules in collisions with helium atoms or with each other, are accelerated with increase in gaseous temperature. Because of a strong temperature dependence for the rate constant of this process, quench of laser generation takes place at a certain gaseous temperature. This factor determines the maximum specific power of CO_2-laser in the end, and the temperature of quench of laser generation appears to be close to 700 K [1]. The maximum specific power which is introduced into the discharge and provides this temperature on the tube axis, equals $P=8\,\mathrm{W\ cm^{-1}}$ in accordance with formula (3.8). Using a typical efficiency of CO_2-laser which is 15%, we arrive at $1\,\mathrm{W\ cm^{-1}}$ for the maximum specific power of laser generation that corresponds to optimal parameters of real laser systems of this type. Notice that according to formula (3.9) the specific laser power per unit length of a discharge tube does not depend on a tube radius. Thus, a simple relationship (3.9) allows us to analyze the temperature difference in a positive column of gas discharge and make reliable estimations.

3.3 Thermal instability of a gas discharge plasma

As known, passage of electric current through a gas discharge leads to a heat release in the bulk which must be compensated by processes of heat transfer. In arc discharges, where heat release can be strong enough, heightened heat transport causes contraction of a plasma region carrying an electric current. Contraction of a discharge leads to an increase in temperature gradients, and therefore enforces heat transfer processes. This thermal character of a gas discharge contraction corresponds to one of the mechanisms of contraction which were considered in the previous section. We shall consider below the peculiarities of this process as applied to the thermal plasma of an arc discharge under conditions of local thermodynamic equilibrium.

Let us analyze the thermal balance equation (3.6). It is convenient to represent this equation in the case at hand in the

form

$$\frac{\mathrm{d}}{\mathrm{d}x}\left(x\,\frac{\mathrm{d}\Theta}{\mathrm{d}x}\right)+A\exp(b\Theta)=0\,. \tag{3.10}$$

Here

$$\Theta=\frac{T-T_0}{T_0}\,,\quad A=\frac{R_0^2pT_0}{4T_0\varkappa T_0}\,,\quad b=T_0\,\frac{\mathrm{d}\ln p}{\mathrm{d}T}\,T_0\,,$$

where T_0 is the wall temperature. We assume therewith that the heat release power p depends on the cross-section of a discharge tube through the gaseous temperature, and that such temperature dependence is sharply defined, i.e. $b\gg 1$. For example, in the case of local thermodynamic equilibrium in an arc discharge plasma we have

$$p\propto N_\mathrm{e}\propto\exp\left(-\frac{J}{2T_\mathrm{e}}\right), \tag{3.11}$$

where N_e is the electron number density, J is the atomic ionization potential. From this it follows that

$$b=\frac{J}{2T_0}\gg 1\,.$$

The solution of equation (3.10) is given by the Fock's formula

$$\Theta=\frac{1}{b}\ln\frac{2\gamma}{Ab(1+\gamma x)^2}\,, \tag{3.12}$$

where γ is the integration constant. In this solution we take account of the boundary condition $\mathrm{d}T/\mathrm{d}\rho=0$ on the axis. The condition $\Theta(x=1)=0$ leads to the following equation for the parameter γ:

$$2\gamma=Ab(1+\gamma)^2\,.$$

As it is seen, the real solution to this equation exists under the condition $Ab<1/2$. Violation of this condition means that the heat removal due to thermal conductivity cannot compensate a thermal release in the bulk. It causes a thermal instability which leads to contraction of a gas discharge. Decrease of a region where heat release takes place promotes to an increase in heat removal that provides the heat balance in a system under consideration.

The threshold of the instability development corresponds to the conditions $\gamma=1$; $Ab=1/2$, i.e. $b\Theta=\ln[2/(1+x)]$. From this we get the following ratio between the specific power of heat release on the axis of a discharge tube p_0 and near their walls $p(T_\mathrm{w})$:

$$\frac{p_0}{p(T_\mathrm{w})}=4\,. \tag{3.13}$$

The electric current radius r_e is defined from the equality of the total power of heat release and heat removal. It gives

$$r_\mathrm{e}^2\sim\frac{\varkappa(T_0)}{\mathrm{d}p/\mathrm{d}T}\,.$$

3.4 Contraction of a gas discharge plasma in the local ionization equilibrium

One can consider in detail the case of developing the above thermal instability under conditions of local ionization equilibrium in a plasma of the positive column of a high-pressure arc discharge. In so doing the analytical expressions for the plasma distribution over the tube cross-section can be obtained that allows us to make the detailed analysis of the problem. Then along with the gaseous thermal conductivity, we take into account the electron thermal conductivity, so that the thermal balance equation (3.6) takes the form

$$\frac{1}{r}\,\frac{\mathrm{d}}{\mathrm{d}r}\left\{r\left[\varkappa(T)\,\frac{\mathrm{d}T}{\mathrm{d}r}+\varkappa_\mathrm{e}(T_\mathrm{e})\,\frac{\mathrm{d}T_\mathrm{e}}{\mathrm{d}r}\right]\right\}+p(r)=0\,. \tag{3.14}$$

Here r is the distance from the discharge tube axis, T, T_e are the gas and electron temperatures, $\varkappa(T)$, $\varkappa_\mathrm{e}(T_\mathrm{e})$ are the coefficients of gaseous and electron thermal conductivity, $p(r)=i(r)\,E$ is the specific power of heat release, so that $i(r)$ is the electric current density, E is the electric field strength. This equation occupies a prominent place in the analysis of an arc discharge plasma and is referred to as Elenbaas–Heller equation [40, 41].

A small parameter of this theory is the ratio of the electron temperature to the atomic ionization potential considering that usually $T_\mathrm{e}\ll J$. Hence, the electron number density depends strongly on the electron temperature, so that in the region where the plasma is concentrated the gas and electron temperatures vary slowly. It allows determination of the distribution of plasma parameters over the tube cross-section by using a small parameter T_e/J.

Let us introduce a reduced parameter

$$y=\frac{\left[T_\mathrm{e}(0)-T_\mathrm{e}(r)\right]J}{2T_\mathrm{e}^2(0)}\,. \tag{3.15}$$

Then according to formula (3.11) we arrive at

$$N_\mathrm{e}(r)=N_\mathrm{e}(0)\,\exp(-y)\,.$$

The power of heat release varies correspondingly over the tube cross-section in the form $p(r)=p_0\exp(-y)$, where $p_0=p(0)$. As it is seen, this function depends strongly on the electron temperature. Hence, in the region which determines the plasma thermal balance, variation of the electron and gas temperatures is insignificant.

With this result let us introduce the parameters

$$\Delta T_\mathrm{e}=T_\mathrm{e}(0)-T_\mathrm{e}(r)\,,\qquad \Delta T=T(0)-T(r)\,. \tag{3.16}$$

The connection between these parameters follows from equation (3.12). Assuming the power-like dependence for the frequency ν of electron-atom collisions on the collisional velocity v: $\nu\propto v^\alpha$, we have

$$\Delta T=\Delta T_\mathrm{e}\,\frac{1+\alpha-\alpha T/T_\mathrm{e}}{2T_\mathrm{e}/T-1}\,. \tag{3.17}$$

Substituting this relationship into equation (3.14) and using a new variable $x=r^2/R_0^2$, we bring this equation to the form:

$$\frac{\mathrm{d}}{\mathrm{d}x}\left[x(\exp(-y)+\xi)\,\frac{\mathrm{d}y}{\mathrm{d}x}\right]-A\exp(-y)=0\,. \tag{3.18}$$

We took into account the fact that the electron thermal conduction coefficient is proportional to the electron number density and separated out this dependence. Parameters of equation (3.18) are given by the formulae

$$\xi=\frac{T\varkappa(T)\,(1+\alpha-\alpha T/T_\mathrm{e})}{\varkappa_\mathrm{e}(T_\mathrm{e})\,(2T_\mathrm{e}-T)}\,,\qquad A=\frac{p_0R_0^2J}{8T_\mathrm{e}^2\varkappa_\mathrm{e}(T_\mathrm{e})}\,. \tag{3.19}$$

Notice that all the parameters of formula (3.19) are taken on the discharge tube axis, and in addition $A \gg 1$.

Equation (3.18) represents the equation of the thermal balance for plasma of a gas-discharge positive column, so that the first term in this equation describes heat removal resulted from gaseous and electron thermal conductivity, and the second term includes heat release due to passage of an electric current through the plasma. Let us consider two regimes of thermal removal successively, so that in the first one the heat removal is determined by gaseous thermal conductivity, and in the second case it is due to electron conductivity. In the first case $\xi \gg 1$, thus one can neglect the term $\exp(-y)$. Then the thermal balance equation takes the form of the Fock's equation (3.10) and has the following solution:

$$y = 2\ln\left(1 + \frac{Ax}{2\xi}\right). \tag{3.20}$$

This corresponds to the following distribution of the electron number density over the tube cross-section:

$$N_e(r) = N_e(0)\,\exp(-y) = \frac{N_e(0)}{(1 + r^2/a^2)^2}\,,$$
$$a^2 = \frac{16T_e^2 T\varkappa(T)\,(1 + \alpha - \alpha T/T_e)}{p_0 J\,(2T_e - T)}\,. \tag{3.21}$$

Integrating over the tube cross-section, we arrive at the total power of heat release per unit length of a discharge tube:

$$P = IE = \int p_0 \exp(-y) 2\pi r\,\mathrm{d}r = \frac{16T_e^2 T\varkappa(T)\,(1 + \alpha - \alpha T/T_e)}{J\,(2T_e - T)}\,. \tag{3.22}$$

In the other limiting case $\xi \ll 1$, we shall consider two ranges of the y-variable change, so that within the first range $y > \ln(1/\xi)$ the solution to equation (3.18) is given by formula (3.20). In the range $y < \ln(1/\xi)$ with introduction of a new variable $Y = N_e(r)/N_e(0) = \exp(-y)$ we bring equation (3.18) to the form:

$$\frac{\mathrm{d}}{\mathrm{d}x}\left(x\,\frac{\mathrm{d}Y}{\mathrm{d}x}\right) + AY = 0\,. \tag{3.23}$$

The solution of this equation with the boundary condition $Y(0) = 1$ is expressed through the Bessel function:

$$Y = J_0\left(2\sqrt{Ax}\right). \tag{3.24}$$

In this limiting case, a plasma region where distribution (3.24) for the electron number density is valid, gives the main contribution to the total discharge current and to the total discharge power. From this it follows for the total discharge power per unit length of a discharge tube:

$$IE = \int p_0 Y 2\pi r\,\mathrm{d}r = 1.36\,p_0 r_0^2\,, \tag{3.25}$$

where the Bessel function is equal to zero at the plasma radius r_0:

$$r_0^2 = 5.78\,\frac{R_0^2}{A} = \frac{12T_e^2\varkappa_e(T_e)}{p_0 J}\,. \tag{3.26}$$

This yields the following expression for the discharge power per unit length of a discharge tube:

$$\frac{P = IE = 16T2_e\varkappa_e(T_e)}{J}$$

Combining expressions (3.19) and (3.27), we get for the heat release power per unit length of a tube for both regimes under consideration:

$$P = IE = \frac{16T_e^2\left[3.4T\varkappa(T)(1 + \alpha - \alpha T/T_e) + 0.24(2T_e - T)\varkappa_e(T_e)\right]}{J(2T_e - T)}\,. \tag{3.28}$$

As it is seen, the thermal balance of the plasma at hand depends weakly on the tube radius because plasma is concentrated near the tube axis. The effective plasma radius is given by formulae (3.21), (3.26) according to which it is inversely proportional to the specific discharge power p_0, i.e. an increase in the specific power of heat release leads to a decrease in the plasma radius.

It is convenient to combine formulae (3.21) and (3.26) for the plasma radius. Let us define the effective plasma radius on the base of the relationship

$$\int N_e(r) 2\pi r\,\mathrm{d}r = 1.36 N_0 r_0^2\,,$$

which holds for the electron distribution described by the Bessel function (3.24). This yields $r_0^2 = 2.31a^2$. Then, sewing together formulae (3.21) and (3.26) with allowance made for the above relationship, we obtain for the effective plasma radius:

$$r_0^2 = 12T_e^2\varkappa_e(T_e)\,\frac{1 + 3.4\xi}{p_0 J}\,. \tag{3.29}$$

As it follows from the above analysis, a gas discharge plasma which is found in a local thermodynamic equilibrium can be described by the theory relying on the ratio of the electron temperature to the atomic ionization potential as a small parameter. Then the distribution of plasma parameters over the cross-section of a discharge tube can be obtained in an analytic form and may be expressed through the electron and gas temperatures on the tube axis. As an illustration of the results of this theory, Table 4 lists parameters of an argon positive-column arc plasma under conditions of local ioniza-

Table 4. Parameters of an argon plasma for the positive column of a high-pressure arc discharge under conditions of local ionization equilibrium.

Parameter	Parameter magnitudes in various conditions					
	1	2	3	4	5	6
T, 10^3 K	2	1	1	2	2	2
T_e, 10^3 K	6	6.5	6.5	7	8	8
Pressure, atm	2	1	3	2	1	2
N, 10^{18} cm^{-3}	7.3	7.3	22	7.3	3.7	7.3
N_e, 10^{14} cm^{-3}	0.71	2.4	4.2	7.1	29	40
w, 10^5 cm s^{-1}	1.58	1.85	1.85	1.77	1.94	1.94
E, V cm^{-1}	6.1	11	33	9.2	6.4	13
ξ	13	1.1	1.9	1.0	0.11	0.15
P, W cm^{-1}	4.1	2.8	2.2	9.7	65	47
I, A	0.67	0.26	0.07	1.1	10	3.7
p_0, W cm^{-3}	11	79	410	180	570	1600
ρ_0, cm	0.36	0.14	0.051	0.17	0.28	0.14
$\eta = \tau_{dif}/\tau_{rec}$	8	7	8	82	930	960

tion equilibrium. Parameters T, T_e, N, N_e, w, and p_0 from this table correspond to a tube axis.

4. Cluster plasma

4.1 Some applications of an arc discharge plasma

Spatially nonuniform plasma under consideration has widespread applications, among which plasmotrons should be primarily mentioned [42, 43]. In plasma generators an arc discharge plasma is used as a heat-transfer agent for many problems of technology, chemistry and metallurgy. Usually, a working object in the form of a powder or dust is introduced in a gas stream which passes through a region of arc discharge. The formed output flow of a hot weakly ionized plasma with an admixture of particles and/or chemically active radicals is ready to use. For example, a plasma flow with small powder particles is played against the treatment of surfaces, and a plasma flow with radicals and excited atomic particles is applied to a production of some chemical compounds. This plasma flow allows one to make the diagnostics of metals on the basis of the emission spectroscopy method. A metal under study is introduced in the process into a gas flow in the form of a dust or solution, and then the gas flow passes through an arc discharge region. Afterglow of excited atoms of metals in an arc plasma allows determination of a relative content of various metals in the object involved.

The occurrence of new directions in science and technology leads to new applications of this plasma. One possibility is correlated here with the production of fullerenes comprising polyatomic carbon molecules in which all the carbon atoms are located on the surface of a sphere or spheroid as the regular hexagons and pentagons [44–46]. Harnessing an arc discharge for this purpose is determined by a high temperature of an arc plasma, by high temperature gradients in the plasma and by a simple procedure of introducing the carbon fragments to plasma as a result of thermal evaporation of graphite electrodes. Carbon fragments resulting from thermal decay of a carbon surface are combinations of hexagon elements of the graphite surface [47]. These fragments may unite into fullerene-like molecules and are swept away to a cold boundary of the plasma region where their hardening occurs. This technology is used both for the production of fullerenes and nanotubes. Furthermore, introduction of some metal powder into graphite electrodes can lead to formation of endohedral molecules [48, 49] which make fullerene molecules with one or several metallic atoms on the inside.

With the aim of demonstrating the applied features of arc plasmas, we shall consider below a cluster plasma making an arc plasma with the metallic clusters incorporated. In this case plasma processes exert some influence on cluster properties. Because the cluster ionization potential falls between the atomic ionization potential and the work function pertaining to a metal surface, clusters are readily ionized in gaseous plasma. This is reflected in the cluster behaviour. In particular, the electrophoresis phenomenon making itself evident in the directional motion of charged clusters occurs in a gas discharge plasma. It results in cluster motion from the anode towards the cathode under the action of the discharge electric field. This phenomenon simplifies introduction of clusters into plasma. First, neutral metallic clusters, which are formed as a result of evaporation of a hot wire and penetrate into a gas discharge plasma through a grid near the anode, are rapidly ionized and propagate over all the plasma volume by the drift and diffusion processes. Second, since clusters make effective emitters, their radiation can determine afterglow of the plasma under consideration. This allows the use of an arc plasma with clusters as a light source. And third, notice a rich chain of processes involving clusters which include mainly the growth and decay of clusters of various sizes. Kinetics of these processes determines the behaviour of the plasma under study and will be considered below.

4.2 Cluster radiation in plasma

Macroscopic particles or clusters introduced into a hot gas can determine, in certain situations, radiative properties of such a system. This effect was discovered in flames as far back as in the last century [50, 51] and it underlies an old idea of a gas-discharge light source with particles as emitters [52]. When analyzing a gas discharge lamp in which radiation is emitted by clusters, let us consider at first some peculiarities of cluster radiation. It should be emphasized that clusters are more effective emitters than other particles in plasma. Indeed, in absence of clusters, plasma radiation results from pair collisions involving electrons. For example, radiation of the Sun photosphere, which mainly contributes to the light intensity reaching the Earth's surface, results from the process

$$e + H \rightarrow H^- + \hbar\omega\,. \tag{4.1}$$

Radiation of powerful arc lamps is determined by photorecombination of electrons and ions in an arc plasma:

$$e + A^+ \rightarrow A^* + \hbar\omega\,. \tag{4.2}$$

These radiative processes possess low effectiveness as they are connected with a small parameter of the system which is the ratio of the electron number density to a typical atomic number density. This small parameter disappears if radiative transitions are made between discrete states of the system as in the cluster case. In going from atoms to molecules and then to clusters, discrete spectral lines of radiation are transformed first into bands, which become continuous in some spectral ranges. Hence, clusters are effective emitters within a continuous spectral range. Comparing gaseous systems with small particles as emitters and bulk radiative systems, one can conclude that in the first case the radiative power is proportional to the total number of atoms in the particles or clusters, whereas in the second case it is proportional to the area at the surface of a macroscopic emitter. Thus, a cluster plasma by its nature is an effective light source.

A cluster can emit radiation in some spectral range, if the latter is active for the cluster, i.e. there appear mechanisms which cause radiative transitions within this spectral range. Metallic clusters under consideration are characterized by a plasma frequency resonance in an optical range:

$$\omega_p = \left(\frac{4\pi N_e^2 e^2}{m_*}\right)^{1/2}, \tag{4.3}$$

where N_e is the electron number density in a conduction zone, m_* is the effective electron mass, e is the electron charge. This resonance causes an effective radiation from heated metallic clusters in the corresponding spectral range.

Radiation of clusters leads to an additional energy loss in a gas discharge plasma. When including this process into the thermal balance of a gas discharge plasma, we can rewrite

balance equation (3.22) in the following form:

$$P = IE = \frac{12\ T_e^2 \varkappa_e(T_e)(1+3.4\xi)}{J} + P_{rad}\,, \tag{4.4}$$

where P_{rad} is the power of plasma radiation which is determined by cluster contribution. Taking the radiative losses into consideration for a given electron temperature on the tube axis, and hence for a given electron number density on the axis, leads to an increase in the volume which is occupied by the plasma. The effective plasma radius accounting for radiative losses is given by the formula

$$r_0^2 = \frac{15 T_e^2 \varkappa_e(T_e)(1+3.4\xi)}{p_0 J} + \frac{P_{rad}}{p_0}\,. \tag{4.5}$$

The other peculiarity of cluster radiation stems from the fact that the cross-section of absorption by a small macroscopic particle of the radius r for photons of the wavelength λ has the form [53]

$$\sigma_{abs} \sim \pi r^2 \frac{r}{\lambda}\,, \tag{4.6}$$

i.e. it is a product of the particle cross-section and a small parameter r/λ. From this it follows that the absorption cross-section for a small particle is proportional to its volume or to a number n of atoms in it. This conclusion is confirmed by measurements of the absorption cross-sections for some metallic clusters (Ag, Li, K) [54–57] which are used below as model ones. Let us represent the absorption cross-section of a cluster in the form of a resonant formula

$$\sigma_{abs}(\omega) = \sigma_0 \Gamma^2 \left[(\hbar\omega - \hbar\omega_0)^2 + \Gamma^2\right]^{-1}\,, \tag{4.7}$$

where Γ is the resonance width, ω_0 is the resonance frequency, σ_0 is the maximum absorption cross-section which is proportional to a number of cluster atoms. The parameters entering this formula have only a weak dependence on the cluster size. A statistical treatment of experimental data [54] for cluster ions Ag_9^+ and Ag_{21}^+ yields $\hbar\omega_0 = 3.9 \pm 0.1$ eV, $\Gamma = 0.59 \pm 0.03$ eV, $\sigma_0/n = (9 \pm 1) \times 10^{-17}$ cm^2; for cluster ions K_9^+ – K_{900}^+ [55, 56] it leads to the following parameters: $\hbar\omega_0 = 2.00 \pm 0.05$ eV, $\Gamma = 0.26 \pm 0.10$ eV, $\sigma_0/n = (34 \pm 6) \times 10^{-18}$ cm^2, and in the case of cluster ions $Li_{139}^+ - Li_{1500}^+$ [57] these parameters are equal to $\hbar\omega_0 = 3.1 \pm 0.1$ eV, $\Gamma = 1.12 \pm 0.15$ eV, $\sigma_0/n = (52 \pm 8) \times 10^{-18}$ cm^2. Below we use these data as model ones for determining the radiative parameters of arc plasmas involving clusters.

Let us go from the absorption cross-sections of clusters to the radiation power of an individual hot cluster. According to the Kirchhoff law, the spectral power of a system radiation $I(\omega)$ is connected with the absorption cross-section of this system by the relationship [58, 59]:

$$I(\omega) = 4\pi c \sigma_{abs}(\omega)\, i(\omega)\,, \tag{4.8}$$

where c is the speed of light, $i(\omega)$ is the spectral radiative power of black body per unit volume and unit solid angle:

$$i(\omega) = \frac{\hbar\omega^3}{4\pi^3 c^3 \left[\exp(\hbar\omega/T) - 1\right]}\,. \tag{4.9}$$

From the above formulae it follows that the total radiation power of a plasma with clusters is proportional to the total cluster mass in a plasma volume and does not depend on the cluster distribution over size. This result is valid also in the case of a hot gas radiation stemming from particles present in gas [58, 60] and follows immediately from theory of radiation as applied to small macroscopic particles; the theoretical findings are confirmed by experimental data for some metal clusters. Below we shall give some parameters of radiation characterizing a gas discharge plasma with clusters by employing the above data for the absorption cross-sections of clusters which are used as model ones.

Table 5 presents the specific power of plasma radiation per unit mass of clusters which is equal to

$$P = \int \frac{I(\omega)\, d\Omega}{M}\,, \tag{4.10}$$

where M is the cluster mass. It is essential that the total power of cluster radiation is proportional to their total mass. Table 6 contains values of the light yield for a gas discharge plasma involving clusters considered. The light yield is given by the formula

$$\eta = \frac{\int I(\omega) V(\omega)\, d\omega}{\int I(\omega)\, d\omega}\,, \tag{4.11}$$

where $I(\omega)$ is the spectral power of cluster radiation, the function $V(\omega)$ characterizes perception of photons of a given wavelength by eye. It has the maximum equal to 683 lm/W at the radiation wavelength $\lambda = 555$ nm. From comparison of data from Table 6 for clusters and black body it follows that metallic clusters possess a more effective spectral parameters as compared to black body; this is due to their transparence to infrared radiation.

Table 5. The specific radiation power P (10^7 W/g) for metallic cluster ions.

Ion	Temperature, 1000 K					
	3.0	3.2	3.4	3.6	3.8	4.0
Li	21	28	38	51	67	87
K	2.8	10	14	20	27	34
Ag	0.64	0.89	1.2	1.7	2.3	3.1

Table 6. The light yield (lm/W) for radiation of metallic clusters.

Ion	Temperature, 1000 K					
	3.0	3.2	3.4	3.6	3.8	4.0
Li	51	63	74	85	94	102
K	108	122	135	146	156	165
Ag	51	62	71	79	84	88
Black body	22	29	36	43	50	57

4.3 Kinetics of processes in a cluster plasma

Clusters introduced in a gas discharge plasma are partially evaporated in consequence of the high temperature. As a result, a vapor consisting of atoms of a cluster material is formed. This vapor makes an admixture to the main gas, and clusters are found in an equilibrium with this vapor. Evolution of clusters in a gas discharge plasma is accompanied by their evaporation and attachment of atoms to them. According to the classical theory of nucleation [61–63], a critical cluster radius exists so that clusters of larger sizes grow and

undersized clusters evaporate. Under conditions in question, the critical radius being determined by the vapor pressure is supported by the evaporation and attachment processes. Clusters can naturally go to walls of the discharge tube as a result of drift and diffusion processes. This determines their lifetime in a discharge tube. But for a high-pressure gas-discharge plasma this lifetime is large enough though it just determines some system parameters. We shall analyze below some kinetic properties of processes which exert influence on the behaviour of metallic clusters in a gas discharge plasma.

Notice that the cluster temperature determining the cluster evaporation time lies between the electron and gas temperatures. In cluster sources of light, optimal cluster temperatures are located within a narrow range, because a low cluster temperature leads to a small radiation power, a high cluster temperature causes prompt cluster evaporation, and parameters of these processes depend strongly on the cluster temperature. Below we shall determine the cluster temperature in a gas discharge plasma on the basis of a simple model [59, 64] according to which atoms and electrons collided with the cluster strongly interact with it. This means that the atom extracts, on average, the energy $3(T_{\rm cl} - T)/2$ from the cluster as a result of their collision, and the electron transfers an average energy $3(T_{\rm e} - T_{\rm cl})/2$ to it, where T, $T_{\rm e}$, $T_{\rm cl}$ are the temperatures of atoms, electrons and clusters, correspondingly, expressed in energy units. Using this model, we obtain the thermal balance equation for a cluster in the form:

$$\frac{3}{2}(T - T_{\rm cl})\, N\bar{v}_{\rm a}\sigma_{\rm a} + \frac{3}{2}(T_{\rm e} - T_{\rm cl})\, N_{\rm e}\bar{v}_{\rm e}\sigma_{\rm e} = \varepsilon_n(\nu_{\rm at} - \nu_{ev})\,. \tag{4.12}$$

Here N, $N_{\rm e}$ are the number densities of buffer gas atoms and electrons, $\bar{v}_{\rm a}$, $\bar{v}_{\rm e}$ are the average velocities of atoms and electrons, correspondingly ($\bar{v}_{\rm a} = \sqrt{8T/\pi m}$, $\bar{v}_{\rm e} = \sqrt{8T_{\rm e}/\pi m_{\rm e}}$, where m is the atomic mass, $m_{\rm e}$ is the electron mass), $\sigma_{\rm a}$ is the cross-section of atom-cluster collision, $\sigma_{\rm e}$ is the cross-section of electron-cluster collision, ε_n is the atomic binding energy for the cluster, $\nu_{\rm at}$ is the frequency of atomic attachment to the cluster surface, and, finally, $\nu_{\rm ev}$ is the frequency of atomic evaporation from the cluster surface. Further we shall assume an occurrence of equilibrium between the processes of growth and evaporation of clusters: $\nu_{\rm ev} = \nu_{\rm at}$. We take the cross-section of atom-cluster collision to be equal to a cluster cross-sectional area $\sigma_{\rm a} = \pi r^2$, where r is a cluster radius, and when evaluating the cross-section of electron-cluster collision, we shall take into account the Coulomb interaction of these particles, so that this cross-section is given by

$$\sigma_{\rm e} = \pi r^2\left(1 + \frac{Ze^2}{rT_e}\right), \tag{4.13}$$

where Z is the cluster charge. From this it follows for the cluster temperature:

$$T_{\rm cl} = \frac{T + \zeta T_{\rm e}}{1 + \zeta}\,, \tag{4.14}$$

where

$$\zeta = \left[1 + \frac{Ze^2}{rT_{\rm e}}\right]\frac{N_{\rm e}}{N}\left(\frac{m}{m_{\rm e}}\right)^{1/2}.$$

As seen, the cluster temperature ranges between the gas and electron ones. As it follows from above expression, a cluster charge exerts some influence not only on its drift motion under the action of electric fields, but also on the cluster temperature.

Let us determine the average cluster charge assuming that clusters are found in local ionization equilibrium with electrons, so that the distribution of clusters over charges is given by the Saha formula. Introduce $P_Z(n)$ — the probability that a cluster consisting of n atoms possesses a charge Z. Then from the Saha formula we have

$$\frac{P_Z(n)\, N_{\rm e}}{P_{Z+1}(n)} = 2\left(\frac{mT_{\rm e}}{2\pi\hbar^2}\right)^{3/2}\exp\left[-\frac{J_Z(n)}{T_{\rm e}}\right], \tag{4.15}$$

where $J_Z(n)$ is the ionization potential of a cluster consisting of n atoms and having a charge Z. For a large metallic cluster we arrive at

$$J_Z(n) = J_0(n) + \frac{Ze^2}{r}\,,$$

where r is a cluster radius. Represent the ionization potential of a neutral cluster in the form:

$$J_0(n) = W_0 + Cn^{-1/3}\,.$$

where W_0 is the metal work function. As a result, we get for the ionization potential of a large cluster:

$$J_Z(n) = W_0 + Cn^{-1/3} + \frac{Ze^2}{r}\,. \tag{4.16}$$

In particular, assuming this formula to be valid for small clusters down to an atom, we apply it to tungsten clusters which will be considered below. From this formula we obtain for the atomic ionization potential: $J_0 = W_0 + C = 7.98$ eV, and the tungsten work function is equal to $W_0 = 4.4$ eV [65, 66]. It yields $C = 3.58$ eV. Let us rewrite formula (4.16) in the form

$$J_Z(n) = W_0 + \frac{C}{n^{1/3}} + \frac{Z\gamma}{n^{1/3}}\,, \tag{4.16a}$$

and in the tungsten case we arrive at $\gamma = e^2 n^{1/3}/r = 9.2$ eV.

It is convenient to define the mean cluster charge Z_n according to the relation $P_Z(n) = P_{Z+1}(n)$. Then we get from above formulae for this quantity:

$$Z_n = \frac{T_{\rm e}n^{1/3}}{\gamma}\ln\left\{\frac{2}{N_{\rm e}}\left(\frac{mT_{\rm e}}{2\pi\hbar^2}\right)^{3/2}\exp\left(-\frac{W_0}{T_{\rm e}}\right)\right\} - \frac{C}{\gamma}\,. \tag{4.17}$$

Table 7 lists some parameters of xenon cluster plasma which consists of a xenon arc plasma with tungsten cluster ions. In particular, an average charge of cluster ions can be found in this table for the mean cluster size equal to $n = 10^3$.

A liquid drop model constitutes a simple and realistic model successfully applied to an account of large metallic clusters. This model allows us to describe various processes with participation of clusters and study their kinetics in gaseous and plasma systems. In particular, within the framework of this model we used above the cross-section of cluster collisions with atoms: $\sigma_{\rm a} = \pi r^2$, where r is a cluster radius. According to the liquid drop model, a cluster radius is connected with a number of atoms in it by the relationship

$n = 4\pi r^3\rho/(3m_a)$. Here ρ is the cluster material density in a bulk system, m_a is the atomic mass. From this one can determine the mobility of cluster ions in plasma within a framework of the Chapman – Enskog approximation:

$$K = 3\sqrt{\pi}\, e \left(8N\sigma_a\sqrt{2Tm}\right)^{-1}, \tag{4.18}$$

where m is the atomic mass for a buffer gas, N is the number density of these atoms. Since the cross-section of atom-cluster collision σ_a is proportional to $n^{2/3}$, the mobility of cluster ions is inversely proportional to $n^{2/3}$. Values of the mobility pertaining to tungsten cluster ions in a xenon arc plasma are given in Table 7 for the cluster size $n = 10^3$ and the discharge regimes at hand.

Table 7. Parameters of an arc xenon plasma with tungsten clusters*.

Parameter	Parameter magnitudes in various conditions					
	1	2	3	4	5	6
p, atm	1	3	2	3	3	3
T, 10^3 K	2	2	2	2	2	2
T_e, 10^3 K	5.5	5.5	5.6	5.6	5.7	5.8
N, 10^{18} cm^{-3}	3.67	11	7.3	11	11	11
N_e, 10^{15} cm^{-3}	0.48	0.84	8.7	1.1	1.4	1.7
E, V cm^{-1}	5.0	15	11	16	17	18
I, A	5.8	1.6	2.8	1.7	1.8	2.0
P, W cm^{-1}	29	25	29	27	31	35
p_0, W cm^{-3}	20	103	77	140	190	260
r_0, cm	1.04	0.42	0.53	0.38	0.34	0.32
$\eta = \tau_{dr}/\tau_{rec}$	9800	4.3×10^4	3.0×10^4	5.2×10^4	6.3×10^4	7 . 6 -
$[W^+]/[W]$	0.095	0.055	0.073	0.059	0.064	$\times10^4$
Z	3.0	2.75	2.88	2.77	2.79	0.070
T_{cl}, 10^3 K	3.45	2.96	3.36	3.17	3.40	2.82
$\mathcal{P}_{rad}$, 10^7 W g^{-1}	9.4	4.1	7.9	6.0	8.6	3.65
w_B, cm s^{-1}	5.3	4.8	5.4	5.2	5.5	13
dm/dt, mg h^{-1}	10	2.9	3.2	1.9	1.3	5.8
η, lm W^{-1}	46	30	43	39	44	0.89
						50

* N, N_e are the number densities of xenon atoms and electrons; T, T_e, T_{cl} are the temperatures of xenon, electrons, and clusters; E, I are the electric field strength and the total discharge current; r_0 is the current radius; $\eta = \tau_{dif}/\tau_{rec}$ is the criterion of a local ionization equilibrium; p_0 is the specific power of heat release on the discharge-tube axis. The following notations are used for parameters of tungsten cluster ions: $[W^+]/[W]$ is a degree of ionization of atomic tungsten vapor; Z is the average charge of tungsten cluster ions; w_B is the mean velocity of tungsten cluster-ions drift towards the cathode. Under conditions studied, one half of energy, which is introduced into discharge, is spent on cluster radiation. Here η is the light yield of the system with allowance made for heat losses in the discharge; dm/dt is the total cluster mass transferred through the discharge in the cathode direction per unit time ($dm/dt = \pi r_0^2 EI/\mathcal{P}_{rad}$, $\mathcal{P}_{rad}$ is the power of cluster radiation per unit cluster mass).

The mobility of tungsten cluster ions determines the cluster drift motion in plasma both in the longitudinal and transverse directions. In particular, let us analyze the motion of cluster ions towards the walls. The transverse electric field strength follows from the condition that the electron flux to the walls reduces to zero on scales of ion fluxes:

$$j_e = -D_e\nabla N_e + eEK_eN_e = 0\,,$$

where D_e is the diffusion coefficient of electrons. Using the Einstein relationship between the diffusion coefficient and mobility ($eD_e = K_eT_e$), we arrive at the transverse electric field strength in a gas discharge plasma: $eE = T_e\nabla N_e/N_e$. Under conditions of local thermodynamic equilibrium, when one can introduce the electron and gas temperatures, this relation takes the form

$$eE = \frac{4T_er^2}{r_0^2(1 + r^2/r_0^2)^3}\,. \tag{4.19}$$

The maximum electric field strength equals $eE_{max} = 2T_e/r_0$. It allows estimation of the maximum drift velocity of cluster ions: $w_{max} = ZKE_{max}$.

Now let us analyze the character of the cluster growth and evaporation processes in a gas discharge plasma. Notice that because clusters are charged, the collisions involving two clusters are insignificant. Therefore, the main processes of the cluster growth and decay proceed according to the scheme

$$A_n + A \rightleftarrows A_{n+1}\,. \tag{4.20}$$

Then, within the framework of the liquid drop model, the frequencies of atomic attachment to a cluster ν_{at} and atomic evaporation from the cluster surface ν_{ev} are defined as follows [59, 69]:

$$\nu_{at} = \sqrt{\frac{8T}{\pi m}}\,\sigma_aN\,;$$

$$\nu_{ev}(t) = \sqrt{\frac{8T}{\pi m}}\,\sigma_aN_{sat}(T)\exp\left[-\frac{\varepsilon_n - \varepsilon_\infty}{T}\right], \tag{4.21}$$

where N is the number density of free atoms of a cluster material, $N_{sat}(T)$ is the number density of atoms in a saturated vapor at a given temperature, σ_a is the cross-section of atomic attachment to the cluster surface which is assumed to be equal to the cluster cross-section, ε_n is the atomic binding energy for a cluster consisting of n atoms, ε_∞ is the atomic binding energy for the corresponding bulk system. Within the framework of a liquid drop model, the atomic binding energy for a cluster is the monotonous function of its size and has the form

$$\varepsilon_n = \varepsilon_\infty - \Delta\varepsilon n^{-1/3}\,. \tag{4.22}$$

According to the liquid drop model of clusters, which is valid for $n \gg 1$, the frequency and rate constant of atomic attachment to a cluster equal [59, 69]:

$$\nu_a = Nk_n\,, \qquad k_n = k_0(T)\xi\, n^{2/3}\,. \tag{4.23}$$

Here ξ is the probability of atomic attachment to the cluster surface as a result of their contact. Evidently, for a large cluster this quantity coincides with that of a bulk surface. The parameter k_0 in formula (4.23) is equal to

$$k_0 = 1.93T^{2/3}m^{1/6}\rho^{-2/3}\,. \tag{4.24}$$

The above expressions form the basis for a quantitative analysis of kinetic properties of a cluster gas-discharge plasma.

Let us consider evolution of clusters in a gas discharge plasma when interacting with their own atomic vapor. Denote the number density of clusters each involving n atoms by N_n. The total number density of atoms entering into the cluster composition equals then $N_{tot} = \sum_n nN_n$. It should be emphasized that equilibrium between processes of clusters evaporation and attachment of atoms to clusters

establishes relatively fast, so that evolution of clusters in their own vapor is determined by evaporation of small clusters and growth of large ones. Let us trace this process. The balance equation for the number density of clusters of a given size has the form

$$\frac{\partial N_n}{\partial t} = Nk_{n-1}N_{n-1} - Nk_nN_n - \nu_nN_n + \nu_{n+1}N_{n+1}\,. \quad (4.25)$$

Here $k_n = k_0(T)\,\xi\, n^{2/3}$ is the rate constant of atomic attachment to a cluster, ν_n is the frequency of cluster evaporation, and once the detailed balance principle is involved we arrive at

$$\nu_{n+1} = k_n(T_{\rm cl})N_{\rm sat}(T_{\rm cl})\exp\left[\frac{\Delta\varepsilon}{T_{\rm cl}n^{1/3}}\right]. \quad (4.26)$$

Using this relation in the balance equation (4.25), we may obtain the equation in the limit $n \gg 1$:

$$\frac{\partial N_n}{\partial t} = -\frac{\partial}{\partial n}\left\{k_0(T)\xi\, n^{2/3}\left[NN_n - N_{\rm sat}(T_{\rm cl})\left(\frac{T_{\rm cl}}{T}\right)^{1/2} \times \exp\left(\frac{\Delta\varepsilon}{T_{\rm cl}n^{1/3}}\right)N_{n+1}\right]\right\}. \quad (4.27)$$

The balance equation for a number density of free atoms has the form

$$\frac{\partial N}{\partial t} = -\frac{\partial}{\partial t}\sum nN_n = \int n\,{\rm d}n\,k_0(T)\xi\, n^{2/3} \times\left[NN_n - N_{\rm sat}(T_{\rm cl})\left(\frac{T_{\rm cl}}{T}\right)^{1/2}\exp\left(\frac{\Delta\varepsilon}{T_{\rm cl}n^{1/3}}\right)N_{n+1}\right] = 0\,. \quad (4.28)$$

Let us analyze the above balance equations by leaning upon the simplest distribution function of clusters over sizes:

$$N_n = A\exp\left(-\frac{n}{\bar n}\right), \quad (4.29)$$

where the normalized constant is $A = N_{\rm tot}/\bar n$. Let us introduce the critical cluster size n_0 for which the integrand comes to zero, and expand the exponent of (4.28) near this point. We have then

$$\int {\rm d}n\,\xi k_0(T)\,n^{2/3}NN_n\left[1 - \exp\left(\frac{\Delta\varepsilon}{T_{\rm cl}n^{1/3}} - \frac{\Delta\varepsilon}{T_{\rm cl}n_0^{1/3}}\right)\right] = \int {\rm d}n\,\xi k_0(T)\,n^{2/3}NN_n\,\frac{\Delta\varepsilon}{T_{\rm cl}}\left[\left(\frac{n}{n_0}\right)^{1/3} - 1\right] = 0\,.$$

From this equation we obtain

$$n_0 = \bar n\left[\frac{\Gamma(5/3)}{\Gamma(4/3)}\right]^3 = 1.033\bar n\,. \quad (4.30)$$

This leads to the following equation for the mean cluster size $\bar n$:

$$\frac{{\rm d}\bar n}{{\rm d}t} = \frac{1}{N_{\rm tot}}\frac{\rm d}{{\rm d}t}\int n^2\,{\rm d}n\,N_n = \frac{1}{N_{\rm tot}}\int n^2\,{\rm d}n\,\frac{\partial N_n}{\partial t} = \frac{1}{N_{\rm tot}}\int {\rm d}n\,\xi k_0(T)\,n^{5/3}NN_n\,\frac{\Delta\varepsilon}{T_{\rm cl}}\left[\left(\frac{n}{n_0}\right)^{1/3} - 1\right] = 0.6\xi Nk_0(T)\,\frac{\Delta\varepsilon}{T_{\rm cl}}\,\bar n^{1/3}\,. \quad (4.31)$$

The solution to this equation yields

$$\bar n = \left(\frac{t}{\tau}\right)^{3/2}, \quad \text{where} \quad \frac{1}{\tau} = 0.4\xi Nk_0(T)\,\frac{\Delta\varepsilon}{T}\,, \quad (4.32)$$

and this allows determination of a typical time of the cluster growth up to its mean size $\bar n$:

$$t_{\rm gr} = \tau\bar n^{2/3}\,. \quad (4.33)$$

To determine a typical cluster size in a gas discharge plasma, it is necessary to equate this time and the lifetime τ_0 of clusters in plasma under conditions considered. It yields

$$\bar n = \left(\frac{\tau_0}{\tau}\right)^{3/2}. \quad (4.34)$$

Thus, evolution of clusters in a gas discharge plasma which results from processes of cluster evaporation and attachment of atoms to clusters, is adequately described on the basis of the liquid drop model for clusters. According to this model, a large cluster with $n \gg 1$ becomes akin to a spherical liquid drop whose density coincides with the density of the corresponding bulk liquid. This model allows us to analyze processes in a gas discharge plasma involving charged clusters and to determine typical parameters of clusters.

4.4 Tungsten clusters in a gas discharge plasma

Properties of a gas discharge plasma involving clusters and evolution of clusters themselves are determined by parameters of these clusters. The latter are compiled in Table 8 for some metallic clusters; they have been resulted from treatment of some parameters of the corresponding bulk systems [66]. We shall enlarge below on clusters of tungsten as the most refractory material. For tungsten clusters, the rate constant k_0 entering formula (4.24) equals $k_0 = 9.1\times10^{-12}\,{\rm cm^3\,s^{-1}}$ at temperature $T = 2000$ K. The probability of attachment of tungsten atoms to a tungsten material surface at their contact is equal to $\xi = 0.566$, as it

Table 8. Parameters of clusters of some refractory metals*.

Metal	$T_{\rm m}$, K	$T_{\rm b}$, K	ε_∞, eV	$\Delta\varepsilon$, eV	Q, eV	p_0, 10^5 atm	W_0, eV
Be	1560	2744	3.02	0.89	3.12	6.1	3.92
Ti	1885	3560	4.25	2.00	4.51	23	3.95
V	2190	4665	4.62	2.30	4.96	85	4.12
Fe	1811	3145	3.6	1.86	3.88	22	4.58
Co	1765	3230	3.90	1.86	4.08	31	4.41
Ni	1728	3070	3.84	1.75	4.12	46	4.50
Cu	1360	2816	3.13	1.35	3.26	7.1	4.40
Pd	1827	3300	3.66	1.79	3.55	2.7	4.8
Ag	1234	2440	2.60	1.25	2.74	5.6	4.3
W	3693	5930	7.99	3.04	7.97	22	4.54
Pt	2045	4100	5.30	2.20	5.33	24	5.32
Au	1333	3150	3.43	1.53	3.58	6.8	4.3

*The following parameters, which are taken for a liquid bulk metal at the melting point, are given in this table: $T_{\rm m}$ is the melting point; $T_{\rm b}$ is the boiling point, i.e. the temperature at which the pressure of saturated vapor is equal to 1 atm; ε_∞, $\Delta\varepsilon$ are the parameters entering formula (4.22); the saturated vapor pressure is determined by formula $p_{\rm sat}(T) = p_0\exp(-Q/T)$; W_0 is the work function of a polycrystal metal. Some discrepancy between the boiling point $T_{\rm b}$ in the table and its value following from formula for the saturated vapor pressure, results from the accuracy of data used and approximation employed.

follows from data for pressures of tungsten saturated vapor and rates of atomic evaporation from the tungsten bulk surface [66] within the temperature range 3000 – 3600 K.

An equilibrium between clusters of different sizes in a gas discharge plasma proceeds through an atomic vapor which arises by cluster evaporation. Under collisions with electrons, this vapor can be partially ionized. The ionization process which transfers a part of the cluster material to an atomic ionized state may be considered as harmful in cluster applications. Hence, under optimal conditions a degree of an atomic vapor ionization must be small that restricts the electron temperature in a gas discharge plasma. The constant of ionization equilibrium for tungsten atomic vapor ($W \rightleftarrows W^+ + e$) is given by the Saha formula:

$$K = \frac{[W^+]\, N_e}{[W]} = \frac{g_e g_i}{g_a} \left(\frac{m_e T_e}{2\pi\hbar^2}\right)^{3/2} \exp\left(-\frac{J}{T_e}\right).$$

Here [X] is the number density of particles of a given sort, the statistical weights are equal to $g_e = 2$ for an electron, $g_i = 12$ for an ion (its ground state is ^4P), and $g_a = 25$ for the tungsten atom (the ground state is ^5D); the ionization potential of the tungsten atom equals $J = 7.98$ eV. Values of this equilibrium constant in the temperature range 5000 – 7000 K are presented in Table 9.

Table 9. The ionization equilibrium constant K (cm^{-3}) for atomic tungsten vapor.

T, 10^3 K	5.0	5.2	5.4	5.6	5.8	6.0
K, cm^{-3}	7.4×10^{12}	1.6×10^{13}	3.3×10^{13}	6.4×10^{13}	1.2×10^{14}	2.1×10^{14}
T, 10^3 K	6.2	6.4	6.6	6.8	7.0	
K, cm^{-3}	3.7×10^{14}	6.1×10^{14}	1.0×10^{15}	1.6×10^{15}	2.4×10^{15}	—

Thus, in the regime of cluster evolution under consideration, clusters are found in an equilibrium with their own atomic vapor. So that processes of the cluster growth and decay regulate the density of atomic vapor, and the distribution function of clusters over sizes results from their interaction with this atomic vapor through the above processes. Since the density of atomic vapor is determined by the cluster temperature, typical times of cluster evolution depends strongly on the cluster temperature. According to formulae (4.32), (4.33) this quantity (for the mean cluster size $\bar{n} = 1000$) yields $t_{gr} = 1.1$ s for $T_{cl} = 3400$ K, $t_{gr} = 0.66$ s for $T_{cl} = 3500$ K, and $t_{gr} = 0.33$ s for $T_{cl} = 3600$ K. These values constitute typical cluster times under conditions studied.

4.5 Cluster source of light

The above analysis shows that a gas-discharge cluster plasma can be used as a light source. We shall discuss below at greater length some prospects of such application. First cluster lamps were constructed by Scholl and collaborators [70 – 73] on the base of clusters of tungsten, rhenium and other refractory materials. Under the action of a microwave discharge of the 100 W in power, a gas discharge plasma is initiated in some small-volume region. In this region clusters of a refractory metal are also generated, and they emit radiation. The maximum light yield for tungsten clusters is 53 lm W^{-1}, and that for rhenium clusters is 62 lm W^{-1}. Though these values are slightly lower than that of best gas-discharge lamps, they exceed remarkably the typical light yields of incandescence lamps (13 lm W^{-1}), i.e. cluster lamps can be of interest in applications. Notice that electron and gas temperatures of cluster lamps are smaller than those of gas-discharge ones. Figure 3 gives spectra of radiation of cluster lamps on the base of clusters of tungsten and rhenium [70 – 73]. The colour temperature of these lamps when using the clusters of tungsten, rhenium and hafnium equals 5100 K, 5500 K and 5600 K, correspondingly, whereas the cluster temperature ranges to 3000 – 4000 K. It is lower in comparison with the colour temperature because spectra of cluster emission are impoverished in infrared radiation as compared to spectrum of black body.

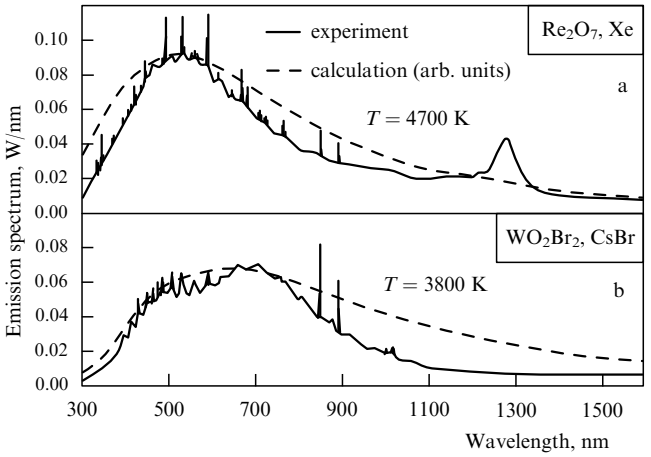

Figure 3. The emission spectra of cluster light sources on the base of Re (a) and W(b).

The principal peculiarity of the cluster lamp realized by Scholl et al. [70 – 73] is the chemical regeneration of a cluster material. In this case, a certain chemical compound is selected wherein a cluster material is transformed at low temperatures; this compound is found in the gaseous phase and does not react with the walls. At high temperatures the compound at hand is separated into its components in such a way that one of the latter features a cluster material. These compounds are WO_2Br_2 in the tungsten case, Re_2O_7 in the rhenium case, MoO_2Br_2 in the case of molybdenum, $HfCl_4$ in the hafnium case and, finally, ZrI_4 in the case of zirconium. There are appropriate chemical compounds for such metals as tantalum, niobium, titanium. At low temperatures the above metal enters into the composition of the gaseous chemical compound, whereas at high temperatures this chemical compound breaks down, and clusters are formed from one of the resultant component. In the tungsten case, the clusters formed consist evidently of WO_2. Thus, in a gas discharge plasma a chemical equilibrium is supported such that gaseous molecules are found in a cold region, and clusters which emit radiation are generated in a hot region. For some refractory metals such as Ir, Pt, Ru, Rh, V, Cr, Mn and Fe, one fails to select appropriate chemical compounds which allow the transfer of these metals to gaseous molecules at low temperatures. Notice that this concept is used also in existing incandescence lamps with a tungsten wire. Here, chemical regeneration of tungsten allows an increase in the wire temperature, i.e. increase in the light yield, and also an increase in the lifetime of these lamps.

This method of chemical regeneration enables conservation of a cluster material from its attachment to walls of a gas-

discharge tube and therefore it is of importance for real cluster lamps. But variations in a chemical content can lead to changes in energetic, kinetic and radiative parameters of the gas-discharge cluster plasma, and this information is required for theoretical analysis of these lamps. Hence, in theoretical modelling of these systems it is convenient to abandon complex schemes of cluster lamps based on chemical regeneration of clusters. Nevertheless, it is necessary to keep in mind such possibilities and use them in the course of experimental modelling on these systems.

As it follows from the above analysis, a cluster lamp is a promising light source. But because it makes a complex technological object, the realization of this problem requires accumulating various information on properties of clusters and bulk of refractory materials. In any case, the experimental [72, 73] and theoretical [74] investigations having been conducted up until this point convince us that cluster lamps offer the promising light sources.

5. Conclusions

The physics of gas discharges ranks among the oldest branches of physical science. Various results in this area have become to be classical and found their places in reference books. Gas discharge has various applications, and now they make up the main aspect of development in gas-discharge physics. But these applied problems are based on understanding the fundamentals of a gas discharge. As an illustration, mention may be made of studies on a nonuniform plasma which are the topic of this paper. Fundamental problems of a nonuniform plasma such as phenomena of contraction of a current region and electrophoresis, provide a basis of study on a cluster plasma, i.e. a gas discharge plasma containing clusters. In addition, this plasma shows specifics which makes it, in particular, to be a promising source of light. Investigation of some features of this plasma is accompanied by solution to new fundamental problems.

The present work was supported by the Russian Fund of Fundamental Research.

References

1. Eletskiĭ A V, Smirnov B M *Fizicheskie Protsessy v Gazovykh Lazerakh* (Physical Processes in Gas Lasers) (Moscow: Energoatomizdat, 1985) [Translated into English (New York: Plenum Press, 1988)]
2. Raizer Yu P *Fizika Gazovogo Razryada* (Gas Discharge Physics) (Moscow: Nauka, 1992) [Translated into English (Berlin: Springer-Verlag, 1991)]
3. Vedenov A A *Fizika Electrorazryadnykh CO_2-Lazerov* (Physics of Electrical Discharge CO_2-Lasers) (Moscow: Energoizdat, 1982)
4. Finkelnburg W, Maecker H, *'Elektrische bögen und thermisches plasma'* Handbuch der Physik, Gruppe 4, Band 22 (Berlin, Heidelberg: Springer-Verlag, 1956) pp. 254-444 [Translated into Russian (Moscow: Inostrannaya Literatura, 1961)]
5. Smirnov B M *Usp. Fiz. Nauk* **164** 665 (1994) [*Phys. Usp.* **37** 621 (1994)]
6. Smirnov B M *Plasma Chem. Plasma Processes* **13** 673 (1993)
7. Smirnov B M *Phys. Scripta* **51** 380 (1995)
8. Eletskiĭ A V, Rakhimov A T *Khimiya Plazmy* **4** 123 (1977)
9. Eletskiĭ A V *Khimiya Plazmy* **9** 151 (1982)
10. Eletskiĭ A V, Chiflikyan R V *Khimiya Plazmy* **15** 266 (1989)
11. Sinkevich O A, Stakhanov I P *Fizika Plazmy* (Plasma Physics) (Moscow: Vysshaya Shkola, 1991)
12. Gieseler H, Grotrian W *Z. Phys.* **25** 342 (1924)
13. Fabrikant V A *Dokl. Akad. Nauk USSR* **24** 531 (1939)
14. Bychkov V L, Eletskiĭ A V *Teplofiz. Vys. Temp.* **17** 1153 (1979)
15. Arutyunyan G G, Galechyan G A *Zh. Tekh. Fiz.* **48** 631 (1978) [*Sov. Phys. Tech. Phys.* **23** 374 (1978)]
16. Eletskiĭ A V 'Kinetic processes in gas lasers', Thesis for Doctorate of Physicomathematical Sciences (Moscow: Kurchatov Institute of Atomic Energy, 1977)
17. Eletskiĭ A V, Smirnov B M *Usp. Fiz. Nauk* **136** 25 (1982) [*Sov. Phys. Usp.* **25** 13 (1982)]
18. Smirnov B M *Iony i Vozbuzhdennye Atomy v Plazme* (Ions and Excited Atoms in Plasma) (Moscow: Atomizdat, 1974)
19. Eletskiĭ A V, in *Fizicheskie Velichiny* (Pod red. I S Grigor'eva, E Z Meĭlikhova) Gl. 18 (Moscow: Energoatomizdat, 1991) [Translated into English *Handbook of Physical Quantities* Ch.18 (Eds I S Grigoriev, E Z Meilikhov) (Boca Raton, NY, London: CRC Press, 1996)]
20. Baranov V Yu, Ul'yanov K N *Zh. Tekh. Fiz.* **39** 249 (1969)
21. Ul'yanov K N *Zh. Tekh. Fiz.* **43** 570 (1973) [*Sov. Phys. Tech. Phys.* **18** 360 (1973)]; Ul'yanov K N, Menakhin L P *Zh. Tekh. Fiz.* **41** 2545 (1971)
22. Bychkov V L, Eletskiĭ A V *Fizika Plazmy* **4** 942 (1978)
23. Eletskiĭ A V, Palkina L A, Smirnov B M *Yavleniya Perenosa v Slaboionizovannoĭ Plazme* (Transfer Phenomena in Weakly Ionized Plasmas) (Moscow: Energoizdat, 1975)
24. Bychkov V L, Eletskiĭ A V, Smirnov B M *Khimiya Plazmy* (Plasma Chemistry) **10** 146 (1983)
25. Eletskiĭ A V, Starostin A N *Fizika Plazmy* **1** 684 (1975)
26. Eletskiĭ A V, Starostin A N *Fizika Plazmy* **2** 838 (1976)
27. Eletskiĭ A V, Kutvitskiĭ V A *Fizika Plazmy* **3** 880 (1977)
28. Frank-Kamenetskiĭ D A *Diffusiya i Teploperedacha v Khimicheskoĭ Kinetike* (Diffusion and Heat Transfer in Chemical Kinetics) (Moscow: Nauka, 1987) [New York: Plenum Press, 1969]
29. Kagan Yu M, Lyagushchenko R I *Opt. Spektr.* **17** 168 (1964) [*Opt. Spectr.* **17** 90 (1964)]
30. Golubovskiĭ Yu B, Kagan Yu M, Lyaguschenko R I *Zh. Eksp. Teor. Fiz.* **57** 2222 (1969) [*Sov. Phys. JETP* **30** 1204 (1970)]
31. Golubovskiĭ Yu B, Lyagushchenko R I *Zh. Tekh. Fiz.* **47** 1852 (1977) [*Sov. Phys. Tech. Phys.* **22** 1073 (1977)]
32. Eletskiĭ A V, Chiflikyan R V, in *Rev. Plasma Chemistry* Vol. 2 (New York: Plenum Press, 1993) p. 317
33. Smirnov B M *Physics of a Weakly Ionized Gas* (Moscow: Mir Publ., 1988)
34. Gurevich A V *Zh. Eksp. Teor. Fiz.* **37** (7) 201 (1959) [*Sov. Phys. JETP* **37** 215 (1960)]
35. Ginzburg V L, Gurevich A V *Usp. Fiz. Nauk* **70** (2) 201 (1960) [*Sov. Phys. Usp.* **3** 115 (1960)]
36. Biberman L M, Vorob'ev V S, Yakubov I T *Kinetika Neravnovesnoĭ Nizkotemperaturnoĭ Plazmy* (Kinetics of Nonequilibrium Low-Temperature Plasmas) (Moscow: Nauka, 1982) [Translated into English (New York: Cons. Bureau, 1987)]
37. Smiths R M M, Prince M *Physica C* **96** 243; 262 (1979)
38. Smirnov B M *Gazorazryadnaya Plazma* (Gas Discharge Plasma) (Moscow: MIPT Publ. 1992)
39. Huxley L G, Crompton W *The Diffusion and Drift of Electrons in Gases* (New York: Wiley, 1974)
40. Hoyaux M F *Arc Physics* (New York: Springer-Verlag, 1968)
41. Neuman W *The Mechanism of the Thermoemitting Arc Cathode* (Berlin: Academic-Verlag, 1987)
42. Semashko N N (Ed.) *Tekhnologicheskie Primeneniya Nizkotemperaturnoĭ Plazmy. Fizika Plazmy* (Moscow: Energoatomizdat, 1983)
43. Tumanov Yu N *Khimiya Plazmy* (Plasma Chemistry) **13** 163 (1987)
44. Krätschmer W et al. *Nature* (London) **347** 354 (1990)
45. Taylor R et al. *J. Chem. Soc. Chem. Commun.* **1423** (1990)
46. Haufler R E et al. *J. Phys. Chem.* **94** 8634 (1990)
47. Eletskiĭ A V, Smirnov B M *Usp. Fiz. Nauk* **165** 977 (1995) [*Phys. Usp.* **38** 935 (1995)]
48. Chai Y et al. *J. Phys. Chem.* **95** 7654 (1991)
49. Johnson R D et al. *Nature* (London) **355** 239 (1992)
50. Faraday M *The Chemical Nature of Candle* (New York: Crowell, 1957)
51. Gaydon A G, Wolfhard H G *Flames, Their Structure, Radiation and Temperature* (London: Chapman and Hall, 1979)
52. Magasa E Japan Patent No. 32-7247 (1957)
53. Landau L D, Lifshitz E M *Electrodynamics of Continuous Media* 2d edition (Oxford: Pergamon Press, 1984)

54. Tiggesbäumker J et al. *Chem. Phys. Lett.* **190** 42 (1992)
55. Brechignac C et al. *Phys. Rev. Lett.* **70** 2036 (1993)
56. Brechignac C et al. *Chem. Phys. Lett.* **164** 433 (1989)
57. Brechignac C et al. *Phys. Rev. Lett.* **68** 3916 (1992)
58. Smirnov B M *Usp. Fiz. Nauk* **163** (7) 51 (1993) [*Phys. Usp.* **36** 592 (1993)]; *Int. J. Theor. Phys.* **32** 1453 (1993)
59. Smirnov B M *Usp. Fiz. Nauk* **164** 665 (1994) [*Phys. Usp.* **37** 621 (1994)]
60. Luizova L A, Smirnov B M, Khakhaev A D *Dokl. Akad. Nauk USSR* **309** 1359 (1989) [*Sov. Phys. Doklady* **34** 1086 (1989)]
61. Frenkel Ya I *Theory of Liquids* (New York: Dover Publ., 1976)
62. Landau L D, Lifshitz E M *Statistical Physics*, Part I, 3rd edition (Oxford: Pergamon Press, 1980)
63. Abraham F F *Homogeneous Nucleation Theory* (New York: Academic Press, 1974)
64. Luizova L A et al. *Teplofiz. Vys. Temp.* **28** 897 (1990)
65. Fomenko V S *Emissionnye Svoĭstva Metallov* (Kiev: Naukova Dumka Publ., 1981)
66. *CRC Handbook of Chemistry and Physics*, 67th ed. (Boca Raton: CRC Press, 1989)
67. Chapman S, Cowling T G *The Mathematical Theory of Nonuniform Gases* (Cambridge: Cambridge University Press, 1952)
68. Ferziger J H, Kaper H G *Mathematical Theory of Transport Processes in Gases* (Amsterdam: North-Holland, 1972)
69. Smirnov B M *Plasma Chem. Plasma Processes* **13** 673 (1993)
70. Weber B, Scholl R *J. Illumin. Eng. Soc.* 93 (Summer 1992)
71. Weber B, Scholl R, in *Physics and Chemistry of Finite Systems: from Clusters to Crystals* (Eds P Jena, S N Khana, B K Rao) (Dordrecht: Kluwer Academic Publ., 1992)
72. Weber B, Scholl R *J. Appl. Phys.* **74** 2274 (1993)
73. Scholl R, Natour G, in *Proc. 22 Int. Conf. Ionized Phen. Gases: Invited Papers* (Eds K H Becker, W E Carr, E E Kunhardt) (New Jersey: Stevens Ins. Technology, 1995)
74. Smirnov B M *Phys. Scripta* **53** 608 (1996)